This is a repository copy of *Evaluation of ion mobility for the separation of glycoconjugate isomers due to different types of sialic acid linkage, at the intact glycoprotein, glycopeptide and glycan level.*.

White Rose Research Online URL for this paper:
http://eprints.whiterose.ac.uk/126084/

Version: Accepted Version

1

Evaluation of ion mobility for the separation of glycoconjugate isomers due to

different types of sialic acid linkage, at the intact glycoprotein, glycopeptide and

glycan level

Albert Barroso[1], Estela Giménez[1,†], Albert Konijnenberg[2], Jaime Sancho[3], Victoria Sanz-

Nebot[1], Frank Sobott[2,4,5,‡]

[1] Department of Chemical Engineering and Analytical Chemistry, University of Barcelona,

Diagonal 645, 08028 Barcelona, Spain

[2] Biomolecular & Analytical Mass Spectrometry group, Department of Chemistry, University of

Antwerp, Antwerp, Belgium

[3] Instituto de Parasitología y Biomedicina "López-Neyra" (IPBLN), CSIC, Armilla, Granada,

Spain

[4]Astbury Centre for Structural Molecular Biology, University of Leeds, Leeds LS2 9JT, United

Kingdom

[5] School of Molecular and Cellular Biology, University of Leeds, LS2 9JT, United Kingdom

Corresponding author: [†]Tel.: +34 934021278; fax: +34 934021233; e-mail address: estelagimenez@ub.edu;

[‡]F. Sobott: e-mail address: f.sobott@leeds.ac.uk

24 **ABSTRACT**

25 The study of protein glycosylation can be regarded as an intricate but very important

26 task, making glycomics one of the most challenging and interesting, albeit under-

27 researched, type of "omics" science. Complexity escalates remarkably when

28 considering that carbohydrates can form severely branched structures with many

29 different constituents, which often leads to the formation of multiple isomers. In this

30 regard, ion mobility (IM) spectrometry has recently demonstrated its power for the

31 separation of isomeric compounds. In the present work, the potential of traveling wave

32 IM (TWIMS) for the separation of isomeric glycoconjugates was evaluated, using

33 mouse transferrin (mTf) as model glycoprotein. Particularly, we aim to assess the

34 performance of this platform for the separation of isomeric glycoconjugates due to the

35 type of sialic acid linkage, at the intact glycoprotein, glycopeptide and glycan level.

36 Straightforward separation of isomers was achieved with the analysis of released

37 glycans, as opposed to the glycopeptides which showed a more complex pattern.

38 Finally, the developed methodology was applied to serum samples of mice, to

39 investigate its robustness when analysing real complex samples.

40

41

1. Introduction

Glycosylation is by far one of the most common and complex posttranslational modifications, with more than half of all secretory and cellular proteins being glycosylated [1–3]. Carbohydrates enhance the functional diversity of proteins, but they can also define their destination or elicit an immune response. The presence of glycans in the surface of eukaryotic cells is vital, as they take part in important cellular events, such as cell–cell interactions and receptor recognition [4]. Notwithstanding its importance and the major role of glycosylation in a multitude of biological processes [5–7], the analysis and characterization of carbohydrates is usually difficult due to their inherent complexity - the main reason why advances in glycomics have been scarcer compared to other "omics" sciences [8,9]. Very often, in contrast to more linearly assembled biological molecules such as proteins or oligonucleotides, carbohydrates can form complex structures, severely branched, with many monosaccharide constituents, which usually results in a multitude of isomers [10].

Mass spectrometry (MS)-based techniques are the prime option for the characterization of glycoproteins, as reliable structural information can be obtained [7,11]. MS is frequently used in conjunction with chromatographic or electrophoretic separation techniques, as this allows high sensitivity profiling and accurate characterisation of heterogeneous glycan structures [12–14]. However, when analysing isomeric glycan structures, MS often fails to separate them [8,15–17], as they have identical mass and atomic composition. Some authors have suggested alternative strategies to separate isomeric glycoconjugates based on their derivatization, the use of capillary electrophoresis (CE) or hydrophilic interaction liquid chromatography (HILIC)[18–23]. But even then, derivatization protocols can be time-consuming, expensive or hinder the

3

66   ionization of some glycans, or, in the case of CE or HILIC, the unambiguous

67   identification is still impossible when different isomers coelute. Moreover, in the last

68   few years, several tandem mass spectrometry (MS/MS) methods have been reported

69   that allow the identification of glycan isomers and the characterization of their structure

70   [24–26]. However, few authors have studied the fragmentation of glycans with different

71   sialic acid linkages. Even then, distinguishing by MS/MS between isomeric glycans due

72   to sialic acid linkage is not trivial and, quite often, is based on differences in the relative

73   abundance of certain fragment ions [27,28]. Therefore, a straightforward technique that

74   helps to separate and differentiate those isomeric compounds is much needed.

75   In this regard, ion-mobility (IM) spectrometry coupled with MS has aroused some

76   interest in the last years, not only in the glycomics field but also in other omics sciences,

77   as a proficient analytical technique for the separation of isomeric compounds

78   [3,8,10,15–17,29–31]. Ion mobility provides an additional dimension for the separation

79   of compounds, where ions are not only separated due to their mass and charge, but also

80   on the basis of their shape and size - thereby resolving ions that would be otherwise

81   indistinguishable solely by MS, such as, for instance, isomers [32–36]. Particularly, IM

82   measures the time (drift time) that a particular ion takes to cross a cell filled with an

83   inert, neutral background gas (N_2 and He are most commonly used) at a controlled

84   pressure under the influence of a weak electric field. The drift time of a specific ion is

85   mainly due to ion-gas collisions; therefore, ions are separated due to their ion-neutral

86   collision cross-section (Ω), related to the overall shape and topology of the ion [32–36].

87   Small compact ions have the shortest drift times, i.e. they arrive first, as a result of their

88   smaller Ω. Moreover, the higher the charge of the ion, the greater the accelerating

89   electric force, and therefore the more quickly the ion will cross the chamber.

90 Consequently, the drift time of an ion is often described as being determined by the

91 collision cross-section-to-charge ratio (Ω/z) [35]. When coupled on-line with MS (IM-

92 MS), ion mobility provides three-dimensional analytical information for each detected

93 species, i.e. shape-to-charge, mass-to-charge and abundance, thus allowing reliable

94 analyte identification.

95 Nowadays, there are several IM methods next to the classical drift-time ion mobility

96 spectrometry (DTIMS), such as field asymmetric waveform ion mobility spectrometry

97 (FAIMS), but among them, traveling wave ion mobility spectrometry (TWIMS) is the

98 one that has seen a major growth in the last years [37,38]. In TWIMS, ions are propelled

99 thanks to a sequence of symmetric potential waves continually propagating through a

100 cell, each ion with its own velocity, thus different species transit the cell in different

101 times. One of the main advantages of TWIMS is that it disperses ion mixtures, allowing

102 the simultaneous measurement of multiple species. This, in conjunction with a high

103 sensitivity obtained when TWIMS is coupled to certain analyzers in MS, such as time-

104 of-flight (TOF), has made this platform an alluring option for structural analysis and

105 isomer separation [38–40]. This platform, along with other IM methods, have been

106 recently explored for the analysis of glycans or glycoconjugates by several authors

107 [8,15,16,41–47].

108 In this work, TWIMS combined with TOF-MS was used for the study of

109 glycoconjugate isomers which differ in the type of sialic acid linkage, with mouse

110 transferrin (mTf) as a model glycoprotein. Sialic acid, an important monosaccharide

111 residue of complex type N-glycans, may form primarily two types of linkages: α2-3 or

112 α2-6. We aim to assess the capacity of TWIMS-TOF-MS (from now on referred to as

113 IM-MS) as an analytical platform to separate α2-3 and α2-6 isomeric glycoconjugates at

114   the intact glycoprotein, glycopeptide and glycan level. The developed methodology was

115   also applied to serum samples of mice, to confirm its robustness when analysing real

116   complex samples.

117

2. Materials and methods

2.1 Chemicals

All chemicals used in the preparation of buffers and solutions were of analytical reagent grade. Isopropanol (iPrOH), hydrochloric acid (HCl, 37% (w/v)), formic acid (FA, 98–100%), ammonium acetate (NH$_4$Ac, ≥98.0%) and glycine (≥99.7%) were supplied by Merck (Darmstadt, Germany). CNBr-activated-Sepharose 4B was provided by GE Healthcare (Waukesha, WI, USA) and "NP-40 alternative" by Calbiochem (Darmstadt, Germany). Sodium chloride (NaCl, ≥99.5%), DL-Dithiothreitol (DTT, ≥99%), sodium cyanoborohydride (NaBH$_3$CN), 2-mercaptoethanol (β-ME), sodium dodecyl sulfate (SDS), iodoacetamide (IAA), ammonium hydrogencarbonate, sodium azide (NaN$_3$, ≥99.5%) water (LC-MS grade), acetonitrile (LC–MS grade) and mouse apotransferrin (mTf, reference: T0523) were supplied by Sigma–Aldrich (St. Louis, MO, USA) and Tris(hydroxymethyl) aminomethane (TRIS, ≥99.5%) by J.T. Baker (Deventer, Holland). Trypsin (Sequencing grade modified) was provided by Promega (Madison, WI, USA). RapiGest® from Waters (Bedford, MA, USA) was used to facilitate the enzymatic digestion. Goat polyclonal antibody against human transferrin (hTf) (immunogen affinity purified) was purchased from Abcam (Cambridge, UK). Human transferrin (hTf) and human α-1-acid glycoprotein (hAGP) were used as additional examples of other glycosylated glycoproteins and were also supplied by Sigma–Aldrich.

2.2 Mice and induction of arthritis

Wild-type (WT) mice were from Harlan Ibérica (Barcelona, Spain). All studies with live animals were authorized by the Institute of Parasitology and Biomedicine "López-Neyra" (IPBLN) and Universidad de Cantabria Institutional Laboratory Animal Care

141 and Use Committees. For the induction of collagen-induced arthritis (CIA), 8-12 weeks-

142 old male mice were immunized as described elsewhere [48,49].

2.3 Purification of serotransferrin from mouse serum samples by immunoaffinity

chromatography (IAC)

145 In order to isolate mTf from the rest of serum proteins, an immunoaffinity (IA)

146 purification was carried out using a cyanogen-bromide sepharose column where a

147 polyclonal antibody against human transferrin (hTf) was bound, as detailed previously

148 [50]. The IA procedure consisted of: first, a conditioning step with two washes of 10

149 mM Tris-HCl; second, approximately 25 μL of serum were diluted 1:8 in 10 mM Tris-

150 HCl (pH 7.6-7.7) in order to improve antigen-antibody interaction, and passed through

151 the column ten times. After washing with 10 mM Tris-HCl and 0.5 M NaCl (pH 7.6-

152 7.7), retained mTf was eluted with 100 mM glycine-HCl (pH 2.5). Eluted mTf was

153 immediately neutralized with 0.5 M Tris. Afterwards, glycine-HCl buffer was

154 exchanged for water by ultracentrifugation, using Microcon YM-10 (MW cut-off 10

155 kDa, Millipore, Bedford, MA, USA). Then, samples were evaporated to dryness using a

156 SpeedVac^{TM} concentrator (Thermo Fisher Scientific, Waltham, MA, USA) and stored at

157 -20ºC until use. Finally, the IA column was washed and stored in 10 mM Tris-HCl and

158 0.01% (w/v) NaN$_3$ (pH 7.6-7.7).

2.4 Analytical approaches for mTf glycosylation study

160 2.4.1   Intact glycoprotein analysis

161 mTf standard (25 μg) was desalted using three different procedures: dialysis, size

162 exclusion and ultracentrifugation. Briefly, in the first method, D-Tube^{TM} dialyzers from

163 Merck-Millipore were left in contact with 100 mM NH$_4$Ac for 15 min. Afterwards, the

8

164 sample was placed into the dialyzer and left in contact with 500 mL of 100 mM NH$_4$Ac

165 for 2 h at 4ºC. Later, the buffer was renewed with 500 mL and the dialysis was allowed

166 to continue for 2 more hours, repeating this process twice. Finally, the sample was

167 carefully recovered and stored at -20ºC until analysis. Regarding the size exclusion

168 procedure, the sample was desalted and the buffer exchanged using Micro Bio-Spin^{TM}

169 columns from BioRad (Hercules, California, USA) following the manufacturer

170 instructions. Columns were centrifuged to remove the excess of packing buffer and

171 washed three times with 500 μL of 100 mM NH$_4$Ac. Finally, the sample was added and

172 collected in a new tube after centrifugation. Lastly, the ultracentrifugation procedure

173 was carried out using Microcon YM-10 (MW cut-off 10 kDa) to desalt and exchange

174 the buffer of the sample. Filters were washed with 100 mM NH$_4$Ac and centrifuged for

175 10 min at 10000 g. Afterwards, the sample was added and washed with 50 μL of 100

176 mM NH$_4$Ac a total of 4 times, centrifuging each time for 10 min at 10000 g. Finally, the

177 final volume was recovered in a new vial after centrifugation for 2 min at 1000 g, and

178 reconstituted to the initial volume (25 μL). Centrifugation procedures were carried out

179 in a MiniSpin® centrifuge (Eppendorf, Hamburg, Germany) at room temperature. In all

180 cases, experiments with the standard glycoprotein were carried out in triplicate and

181 intact mTf in 100 mM NH$_4$Ac was injected directly into the mass spectrometer under

182 non-denaturing conditions and detected in positive ion mode.

183 2.4.2   Glycopeptide analysis

184 mTf standard (25 μg) was reduced, alkylated and immediately subjected to trypsin

185 digestion in the presence of RapiGest® as explained in previous work [51]. Briefly, a

186 solution of 0.5 M DL-dithiothreitol (DTT) in 50 mM NH$_4$HCO$_3$ was added to an aliquot

187 of mTf with 0.1% (w/v) RapiGest®. The mixture was incubated at 56ºC for 30 min and

188 then alkylated with 50 mM iodoacetamide (IAA) for 30 min at room temperature in the

189 dark. Excess reagent was removed by ultracentrifugation with Microcon YM-10

190 columns (Millipore, Bedford, MA, USA). The final residue was recovered from the

191 upper reservoir and reconstituted with NH_4HCO_3 buffer with 0.1% RapiGest®. Trypsin

192 in a 1:40 ratio was added and the mixture was incubated overnight at 37ºC. Afterwards,

193 the surfactant was hydrolyzed to avoid MS incompatibilities as follows: formic acid

194 (FA) was added to the digest to a final concentration of 5% (v/v) and the mixture was

195 incubated in the digester at 37ºC for 30 min. Then, the solution was centrifuged to

196 separate RapiGest® residues. mTf tryptic digests were stored at -20ºC until analysis. All

197 the experiments with the standard glycoprotein were carried out in triplicate.

198 For the analysis of glycopeptides, a Waters Nano ACQUITY UPLC® was used with a

199 double binary gradient pump, using a peptide BEH C18 column (1.7 µm particle

200 diameter, 130 Å pore, 100 x 0.1 mm length x ID; Waters). Experiments were performed

201 at room temperature with gradient elution at a flow rate of 400 nL min^{-1}. Eluting

202 solvents were A: water with 0.1% (v/v) of formic acid (FA), and B: acetonitrile with

203 0.1% (v/v) FA. Solvents were degassed by sonication (10 min) before use. The

204 optimum elution program was: solvent B from 10 to 60% (v/v) within 20 min as linear

205 gradient, followed by cleaning and re-equilibration steps of B: 60 to 100% (v/v) (5

206 min), 100% (v/v) (5 min), 100 to 10% (v/v) (5 min) and 10% (v/v) (5 min). Before

207 analysis, samples were filtered using a 0.22 μm polyvinylidene difluoride centrifugal

208 filter (Ultrafree-MC, Millipore, Bedford, MA, USA) centrifuging at 10,000 g for 4 min.

209 Sample injection (300 nL) was performed with an autosampler refrigerated at 4ºC.

210 Control of the instrument was performed using MassLynx 4.1 (Waters).

211 2.4.3   Glycan analysis

212 IAC purified mTf or mTf standard (25 μg) was reduced with 0.5% 2-mercaptoethanol

213 (β-ME) and 0.5% SDS in 50 mM NH_4HCO_3 (pH 7.6-7.7) and heated in a thermo block

214 at 100 ºC for 30 min [19]. Once the sample was at room temperature, a volume of 50

215 mM NH_4HCO_3 (pH 7.6-7.7) with 1% (v/v) of NP-40 alternative was added to obtain a

216 final concentration of 0.1% SDS and β-ME in the sample. To release the N-glycans,

217 1μL of PNGase F (1 U) solution was added to the mixture, which was afterwards

218 incubated at 37ºC for 18 h. Digestion was stopped by heating the sample in a thermo

219 block at 100ºC for 5 min. Then, released glycans were isolated by solid phase extraction

220 (SPE) using Hypercarb cartridges (25 mg, 1 mL volume, Thermo Fisher Scientific) and,

221 subsequently, purified by ice-cold acetone precipitation following the procedure

222 reported in [19] in both cases. Reduced glycans were diluted with 50:50 H_2O/ACN with

223 0.1% FA and directly analyzed by IM-MS in negative ion mode. All the experiments

224 with the standard glycoprotein were carried out in triplicate. Mice derived transferrin

225 glycan analysis was carried out in duplicate, including purification and release of

226 glycans.

227 **2.5 Ion mobility-mass spectrometry**

228 For IM-MS analysis a Synapt G2 HDMS instrument from Waters was used. Samples

229 were directly introduced into the mass spectrometer using home-made nano-

230 electrospray ionization (nano-ESI) gold-coated borosilicate capillaries; unless when

231 analysed by nano-UPLC-IM-MS, in which case an in-line nano-ESI interface with

232 commercially available coated needles was used.

233 Spectra were acquired in positive mode for the analysis of intact glycoproteins and

234 glycopeptides, and in negative mode for glycans, and conditions were optimized in each

235 case. The voltages for spray capillary, sampling cone, trap collision energy (CE), trap

236　direct current (DC) bias and transfer CE were, respectively: intact glycoproteins, 1.4-1.6

237　kV, 30 V, 4 V, 40 V and 0 V; glycopeptides, 1.5-1.7 kV, 50 V, 4 V, 20 V and 0 V; and

238　glycans, 1.5 kV, 50 V, 4 V, 45 V and 0 V. The "trap CE" voltage was only increased to

239　60 V when fragmentation of the glycopeptides was the goal. Mass spectrometer control

240　and spectra processing were carried out using MassLynx 4.1 (Waters).

241　The software IMoS [52,53], available for free at imospedia.com, was used for the

242　theoretical calculations of the collision cross sections (CCS) of glycans, using their

243　minimum energy structures. The online tool carbohydrate builder, available at

244　glycam.org [54], was used to generate the required input for theoretical calculations.

245　The tool allows building different glycan isomers based on monosaccharide unit and

246　linkage type, and generates minimum energy structures.

247

3. Results and discussion

3.1   Intact glycoprotein analysis

It is well established that intact proteins can be analysed mainly in two different ways when using electrospray ionization: under denaturing or non-denaturing (i.e., "native") conditions. In the first case, the protein appears highly charged with a broad charge state distribution; thus, the separation of the different glycoforms is difficult. On the other hand, an advantage of native MS is that it strongly reduces charging, hence the different glycoforms can be more clearly resolved [55].

Using native MS in this work, the concentration of ammonium acetate and the nano-ESI source parameters were optimized to improve and obtain the best possible sensitivity and separation between mTf glycoforms in positive ion mode. Moreover, in order to obtain an acceptable separation between the several glycoforms, mTf was washed repeatedly with 100 mM NH_4Ac to eliminate excipients and salts, and injected directly into the mass spectrometer without further separation. Without washing, no glycoform separation was observed whatsoever. Three methods were evaluated to desalt the glycoprotein: dialysis, size exclusion and ultracentrifugation, with the latter one giving the best results (see supplementary Figure S1). Afterwards, the drift times of intact glycoforms were determined by ion mobility. In Figure 1-a, the ion with charge +19 of mTf is shown, as well as the arrival time distributions (ATD) of different sections of this peak (Figure 1-a (i-v)), each corresponding to one intact glycoform of mTf). As can be observed in the ATD profiles, only one, relatively wide peak is obtained for each glycoform. Hence, these results imply that, at least for large glycoproteins with a low degree of glycosylation, the glycan part has barely any influence on the overall size of the whole molecule as the CCS appears virtually unaffected by glycosylation. hTf and

13

272   hAGP were also studied to see if the same behaviour was observed with other

273   glycoproteins. Figure 1-b and 1-c show the separation between intact glycoforms in the

274   MS spectra of hTf (for the ion with charge +19) and hAGP, respectively. As can be

275   observed, the peak was better resolved for hTf, but no separation was observed for

276   hAGP, as the number of glycoforms was considerably higher and the overlapping of

277   several ion distributions was unavoidable. Moreover, one wide peak was observed again

278   when the drift time of each section of the mass spectrum was measured for both

279   glycoproteins. Regarding hTf, each section corresponded to one glycoform (Figure 1-b

280   (i-iv)), whereas, in the case of hAGP, the resolution was not high enough to ensure that

281   a selected region of the peak corresponded to one defined glycoform (Figure 1-c (i-v)),

282   because of the high glycosylation degree of hAGP. The higher the m/z region of this

283   peak however, the bigger the carbohydrate fraction is (usually meaning more complex

284   and branched glycans). This is due to the fact that an increase of m/z within the same

285   charge state can only be due to an increase in the number of glycan subunits of the

286   carbohydrate fraction, as the polypeptide backbone remains unaltered. For the sake of

287   consistency, we will refer to each section of the peak as glycoform, even if, as in the

288   case of hAGP, they are not resolved. Interestingly, the drift time increased with

289   increasing carbohydrate fraction, i.e. complexity and branching of the glycoforms, in all

290   three cases (see Figure 1-a (i-v), 1-b (i-iv) and 1-c (i-v), type of glycoform indicated

291   where possible). The relative drift time differences between glycoforms were higher in

292   proteins with higher glycosylation content, as can be observed for hAGP (see Figure 1-

293   c). Moreover, if we compare the drift time between different glycoforms of mTf and

294   hTf, the increase in drift time was more noticeable in hTf, as the percentage of

295   glycosylation is slightly higher here in relation to the total protein mass. As Table 1

296   shows, for the same relative increase in m/z, the relative drift time increase is higher for

14

297 hAGP, which demonstrates that for glycoproteins with a high percentage of

298 glycosylation, differences in the glycosylation have a greater effect on the drift time of

299 the whole molecule (i.e., they significantly alter the CCS of the whole glycoprotein). It

300 could then also be conceivable to separate isomers due to the different sialic acid

301 linkage (of the same glycoform) at the intact protein level if the glycan:peptide ratio was

302 high enough. However, this option would not have been viable for all types of

303 glycoproteins, thus, other alternatives were studied.

304 **3.2 Glycopeptide analysis**

305 As mTf only shows one glycosite at asparagine 494, only one glycopeptide is expected

306 after tryptic digestion (N_{494} glycopeptide, peptide: NSTLCDLCIGPLK). However, with

307 the direct injection of the digest, the N_{494} glycopeptide was not detected, hence, an

308 additional separation before the MS was mandatory. In this regard, nano-UPLC was

309 used as a separation technique prior to IM-MS detection, in order to separate the

310 glycopeptide from the other peptides and simultaneously determine the drift time of the

311 different glycoforms. Injection volume, flow rate and gradient were optimized to obtain

312 the best sensitivity with a stable spray (see section 2.4, Materials and Methods). Table 2

313 shows the detected glycoforms at the peptide level, their theoretical and experimental

314 masses, mass error and observed charge states.

315 Regarding the determination of the drift time of the different glycopeptide glycoforms,

316 even though a range of different values for the wave velocity (WV) and wave height

317 (WH) of the TWIMS device were tested, only one drift time value was observed. This

318 suggests that no isomer separation was possible at this mobility resolution, which is

319 probably due to the fact that the different isomers had similar CCS despite the distinct

320 orientation of the sialic acid. Recently, Hinneburg et al. [15] and Guttman et al. [45]

15

also described this observation analysing glycopeptides directly by IM-MS. They observed no isomeric separation, unless fragmentation of the glycopeptide was carried out and one of the observed smaller fragments still contained the sialic acid. This fragment (obtained before the IM cell) had different drift times depending on the sialic acid linkage, because a change in the orientation of the sialic acid was more noticeable (i.e. the CCS was more affected) in a smaller analyte. We also tested this approach, by fragmenting the most intense glycopeptide glycoform (N(H5N4S2)STLCDLCIGPLK) before the IM cell. Figure 2-a shows the collision induced dissociation (CID) MS/MS spectrum for this glycoform. Several fragments were obtained, e.g., the glycolylneuraminic acid (S1) and H1N1 and H2N1 fragments. Among all the fragments however, H1N1S1 was the one that still retained the sialic acid linkage and had enough intensity to yield a good and accurate drift time measurement. Isomer separation was observed in the aforementioned glycan fragment. Specifically, as it is shown in Figure 2-c, two drift time peaks were clearly observed at this m/z, which are postulated to be due to the sialic acid being α2-6 and α2-3 linked. To confirm that the sialic acid is the monosaccharide that affects the CCS of the fragment the most, the ATD of the fragment H1N1 is shown in supplementary Figure S2-c. In this case, we only observed one drift time, which demonstrates that it is the sialic acid which causes observable CCS differences seen as two different drift times of the fragment H1N1S1.

Moreover, in order to confirm that the distinct drift times observed for the glycan fragment could be due to different sialic acid linkages, the theoretical CCS of the H1N1S1 isomers were calculated. The obtained CCS values can be found in Table 3. The CCS for the two H1N1S1 were different enough to be separated by IM. Taking into account the CCS values of Table 3, the more prominent, lower drift time peak (i.e.,

345   lower CCS) should correspond to the α2-6 glycan, whereas the second peak represents

346   the α2-3 glycan.

347   Our results are in accordance with those obtained by Hinneburg et al. [15], who, using

348   modelling, drew the same conclusions. This is also in agreement with Guttman et al.

349   [45], who found that biantennary glycoforms showed lower content of α2-3 sialylation.

350   In our case, the percentage of α2-3 glycan was approximately 14% (taking into account

351   the measured area of each drift time peak, see Figure 2-c). However, this ratio can vary

352   depending on the glycoprotein studied [45]. This glycopeptide approach, through the

353   analysis of the fragment H1N1S1, gave valuable information about the content of each

354   type of sialic acid as the fragment H1N1S1 came from both branches of the H5N4S2

355   glycopeptide (we did not detect any fragment with only one antenna remaining (H3N3

356   or H3N3S1), suggesting that both antennas might indeed be fragmented). This relevant

357   information could permit, in the future, to correlate changes in protein sialylation with

358   specific disease biomarkers which involve protein glycosylation, such as, e.g., in cancer

359   or inflammation.

360

361   **3.3 Glycan analysis**

362   Finally, we proceeded with the study of the enzymatically released glycans using

363   PNGase F. Different solvents were tested to obtain the best spray and ionization yield,

364   and a slightly superior glycan signal was obtained at 50:50 H_2O:ACN with 0.1% FA.

365   Table 4 shows the detected mTf glycans along with their theoretical and experimental

366   masses, mass error and observed charge states. In Figure 3 the ATD profile of H5N4S2

367   glycans at different values of WV and WH is shown. Two peaks are observed which are

believed to correspond to two different isomers of the glycan H5N4S2, in analogy to the previously obtained results (Figure 2-c) with the fragment H1N1S1 of the glycopeptide N(H5N4S2)STLCDLCIGPLK. Fine tuning of the IM parameters was mandatory in order to resolve both drift time peaks. A WV value of 450 m s^{-1} and WH of 25 V was selected as optimal for the analysis of all mTf glycans. It is worth mentioning that in this case, glycans were analyzed in negative mode and, as can be observed in Figure 3, the first isomer was clearly the less abundant one. This is in contrast to the glycopeptide analysis which was done in positive mode, where the less abundant isomer was the second one. This could be due to the fact that both molecules were, actually, quite different - specifically, the glycan had eleven monosaccharide units, as opposed to the fragment observed in the glycopeptide analysis which had only three. With regard to other glycans, three different peaks, i.e., three drift times, were observed for H6N5S3 (see supplementary Figure S3-c), albeit separation was slightly worse than observed for H5N4S2. H5N4S1 on the other hand only showed one wide peak (see supplementary Figure S3-d), implying that only one glycan isomer exists or that the different isomers have similar CCS, and IM is not able to distinguish them (as the absence of other drift time peaks does not preclude the presence of other isomers). It is also worth pointing out that when the glycan contained a fucose unit, the isomeric separation was somewhat hampered, as observed in supplementary Figure S3-b. We reckon that the addition of one extra monosaccharide unit might affect the global CCS of the glycan, and as the whole glycan is bigger, a small variation in the orientation of the sialic acid is less noticeable.

To confirm that separation of isomeric glycans due to the sialic acid linkage was also possible with other glycoproteins, hAGP was also digested with PNGase F and the

392   released glycans analysed by IM-MS. Separation of isomeric glycans was achieved,

393   seemingly obtaining the same results as with mTf. As an example, the arrival time

394   distributions of the H5N4S2 and H6N5S2 glycans are shown in supplementary Figure

395   S4. As can be seen, two drift time peaks were obtained for the H5N4S2 glycan and

396   three peaks for H6N5S3, albeit separation was poorer in both cases when compared to

397   mTf.

398   Moreover, to confirm that ion mobility separation of these possible isomers is due to

399   different sialic acid linkages, Table 3 shows the theoretical CCS values of the four

400   possible isomers for the glycan H5N4S2. The differences between these calculated

401   values suggest that the observed ion mobility peaks could be due to isomeric glycans

402   with different types of sialic acid linkage. With the knowledge of theoretical CCS, and

403   the abundance of the α2-3 H1N1S1 fragment being lower than α2-6 (based on

404   fragmentation of the H5N4S2 glycopeptide, see above), some conclusions can be

405   drawn. We reckon that the presence of the isomer with two sialic acids α2-3 can be

406   discarded and that the two peaks observed must correspond to the isomers with higher

407   content in α2-6, that is, the isomer with two sialic acids α2-6 and the isomer with one

408   sialic acid α2-6 and one α2-3 (although we cannot specify the branch where each sialic

409   acid is located). Alternative approaches for the study of isomeric glycoconjugates, for

410   instance using specific sialidases [18], would however allow to obtain complementary

411   information and reliably assign the different peaks to the corresponding isomers.

412   **3.4 Mouse serum sample**

413   To further asses the ability of the established method to separate isomeric

414   glycoconjugates in biological samples, we measured the drift time of mTf glycans

415   purified from serum samples. Only the analysis of the released glycans by IM-MS was

416   included in this study, as it was found to be the most sensitive and straightforward

417   approach to obtain information about isomeric forms. Two serum samples were

418   analysed: one healthy control and one sample with collagen-induced arthritis (CIA), an

419   autoimmune disease known to alter the glycosylation pattern of mTf [51,58]. As can be

420   seen in Figure 4, two peaks were observed for H5N4S2 glycan and three peaks for

421   H6N5S3 in both samples, with the same drift time and similar relative intensities as in

422   the mTf standard (compare Figure 4 with supplementary Figure S3). Although

423   additional samples are required to observe possible differences in the relative abundance

424   of glycan isomers between control and pathological samples, the presented

425   methodology shows great potential for the separation of isomeric glycans and the

426   discovery of novel biomarkers in glycomic studies.

427

428   4. Concluding remarks

429   In the present paper, the capability of IM-MS to separate isomeric glycoconjugates

430   which are due to different types of sialic acid linkage (i.e. α2-3 and α2-6) has been

431   evaluated at three different levels: intact glycoprotein, glycopeptides, and the released

432   glycans. Separation of isomeric glycoconjugates is an important task in the glycomics

433   field, because it has been reported that differences in the abundance of some glycan

434   isomers might be of great importance for the early diagnosis or control of, for instance,

435   inflammatory diseases and certain types of cancer.

436   With our current knowledge of glycosylation effects on molecule size, and the limited

437   ability of Synapt IM-MS instrumentation to resolve small CCS differences, isomeric

438   separation cannot be obtained at the intact glycoprotein and glycopeptide level.

439   Released glycans however can be separated after optimization of the IM parameters. As

440 stated before by others [15,45], and also demonstrated in this work, there is a

441 workaround to distinguish different types of sialic acid linkage in glycopeptides that

442 takes into account the mobility of an MS/MS fragment which still retains the sialic acid.

443 This method can however be time-consuming and rather difficult, as glycopeptides must

444 be separated from the rest of the digest and, besides, the obtained glycopeptide fragment

445 is, actually, a glycan.

446 The interest in using ion mobility for glycoconjugate separation and identification has

447 seen a major growth in the last years. Thus, it is likely that new technologies and

448 improvements will become available soon, including the advent of ion mobility

449 instrumentation with up to ten times higher resolution. Therefore, the separation of

450 sialic acid linkage isomers may also become possible at the level of glycopeptides and

451 intact proteins in the future.

452

453

460

5.   References

[1]   A.P. Corfield, M. Berry, Glycan variation and evolution in the eukaryotes, Trends Biochem. Sci. 40 (2015) 351–359.

[2]   H.A. Abbass, H.A. El Hassan, H. Bahmad, A. Zebian, R. Youssef, J. Ismail, R. Zhu, S. Zhou, X. Dong, M. Nasser, M. Bahmad, H. Darwish, Y. Mechref, F. Kobeissy, Glycosylation and other post translational modifications alterations in neurodegenerative diseases: current status and future role in neurotrauma, Electrophoresis. 37 (2016) 1549–1561.

[3]   F. Zhu, J.C. Trinidad, D.E. Clemmer, Glycopeptide Site Heterogeneity and Structural Diversity Determined by Combined Lectin Affinity Chromatography/IMS/CID/MS Techniques, J. Am. Soc. Mass Spectrom. 26 (2015) 1092–1102.

[4]   A. Grigorian, S. Torossian, M. Demetriou, T-cell growth, cell surface organization, and the galectin glycoprotein lattice, Immunol. Rev. 230 (2009) 232–246.

[5]   R.A. Dwek, Glycobiology: towards understanding the function of sugars, Chem. Rev. 96 (1996) 683–720.

[6]   P.M. Rudd, T. Elliott, P. Cresswell, I.A. Wilson, R.A. Dwek, Glycosylation and the immune system, Science (80-.). 291 (2001) 2370–2376.

[7]   H.J. Allen, E.C. Kisailus, eds., Glycoconjugates: Composition: Structure, and Function, CRC Press, 1992.

[8]   J. Hofmann, H.S. Hahm, P.H. Seeberger, K. Pagel, Identification of carbohydrate anomers using ion mobility-mass spectrometry, Nature. 526 (2015) 241–244.

[9]   K. Mariño, J. Bones, J.J. Kattla, P.M. Rudd, A systematic approach to protein glycosylation analysis: a path through the maze, Nat. Chem. Biol. 6 (2010) 713–723.

[10]   K. Pagel, D.J. Harvey, Ion Mobility − Mass Spectrometry of Complex Carbohydrates: Collision Cross Sections of Sodiated N-linked Glycans, Anal. Chem. 85 (2013) 5138–5145.

[11]   N. Leymarie, J. Zaia, Effective use of mass spectrometry for glycan and glycopeptide structural analysis, Anal. Chem. 84 (2012) 3040–3048.

[12]   M.L.M. Hennrich, A.A. Gavin, Quantitative mass spectrometry of posttranslational modifications: Keys to confidence, Sci. Signal. 8 (2015) 1–5.

495   [13]   M. Wuhrer, Glycomics using mass spectrometry, Glycoconj. J. 30 (2013) 11–22.

496   [14]   Y. Zhang, J. Jiao, P. Yang, H. Lu, Mass spectrometry-based N-glycoproteomics

497   for cancer biomarker discovery, Clin. Proteomics. 11 (2014) 18.

498   [15]   H. Hinneburg, J. Hofmann, W.B. Struwe, A. Thader, F. Altmann, D. Varón Silva,

499   P.H. Seeberger, K. Pagel, D. Kolarich, Distinguishing N-acetylneuraminic acid

500   linkage isomers on glycopeptides by ion mobility-mass spectrometry, Chem.

501   Commun. 52 (2016) 4381–4384.

502   [16]   D.J. Harvey, C.A. Scarff, M. Edgeworth, M. Crispin, C.N. Scanlan, F. Sobott, S.

503   Allman, K. Baruah, L. Pritchard, J.H. Scrivens, Travelling wave ion mobility and

504   negative ion fragmentation for the structural determination of N-linked glycans,

505   Electrophoresis. 34 (2013) 2368–2378.

506   [17]   P. Both, A.P. Green, C.J. Gray, R. Šardzík, J. Voglmeir, C. Fontana, M. Austeri,

507   M. Rejzek, D. Richardson, R.A. Field, G. Widmalm, S.L. Flitsch, C.E. Eyers,

508   Discrimination of epimeric glycans and glycopeptides using IM-MS and its

509   potential for carbohydrate sequencing, Nat Chem. 6 (2014) 65–74.

510   [18]   M. Mancera-Arteu, E. Giménez, J. Barbosa, V. Sanz-Nebot, Identification and

511   characterization of isomeric N-glycans of human alfa-acid-glycoprotein by stable

512   isotope labelling and ZIC-HILIC-MS in combination with exoglycosidase

513   digestion, Anal. Chim. Acta. 940 (2016) 92–103.

514   [19]   E. Giménez, M. Balmaña, J. Figueras, E. Fort, C. Bolós, V. Sanz-Nebot, R.

515   Peracaula, A. Rizzi, Quantitative analysis of N-glycans from human alfa-acid-

516   glycoprotein using stable isotope labeling and zwitterionic hydrophilic

517   interaction capillary liquid chromatography electrospray mass spectrometry as

518   tool for pancreatic disease diagnosis, Anal. Chim. Acta. 866 (2015) 59–68.

519   [20]   R.B. Parker, J.E. McCombs, J.J. Kohler, Sialidase specificity determined by

520   chemoselective modification of complex sialylated glycans, ACS Chem. Biol. 7

521   (2012) 1509–1514.

522   [21]   P. Jackson, M.I. Attalla, N-Nitrosopiperazines form at high pH in post-

523   combustion capture solutions containing piperazine: a low-energy collisional

524   behaviour study, Rapid Commun. Mass Spectrom. 24 (2010) 3567–3577.

525   [22]   F. Tousi, J. Bones, W.S. Hancock, M. Hincapie, Differential chemical

526   derivatization integrated with chromatographic separation for analysis of

527   isomeric   sialylated   N-glycans: a   nano-hydrophilic   interaction   liquid

528   chromatography-MS platform, Anal. Chem. 85 (2013) 8421–8428.

[23]   G.S.M. Kammeijer, B.C. Jansen, I. Kohler, A.A.M. Heemskerk, O.A. Mayboroda, P.J. Hensbergen, J. Schappler, M. Wuhrer, Sialic acid linkage differentiation of glycopeptides using capillary electrophoresis − electrospray ionization − mass spectrometry, Sci. Rep. 7 (2017) 3733.

[24]   A. V. Everest-Dass, J.L. Abrahams, D. Kolarich, N.H. Packer, M.P. Campbell, Structural feature ions for distinguishing N- and O-linked glycan isomers by LC-ESI-IT MS/MS, J. Am. Soc. Mass Spectrom. 24 (2013) 895–906.

[25]   E. V. Da Costa, A.S.P. Moreira, F.M. Nunes, M.A. Coimbra, D. V. Evtuguin, M.R.M. Domingues, Differentiation of isomeric pentose disaccharides by electrospray ionization tandem mass spectrometry and discriminant analysis, Rapid Commun. Mass Spectrom. 26 (2012) 2897–2904.

[26]   S. Zhou, X. Dong, L. Veillon, Y. Huang, Y. Mechref, LC-MS/MS analysis of permethylated N-glycans facilitating isomeric characterization, Anal. Bioanal. Chem. 409 (2017) 453–466.

[27]   S.F. Wheeler, D.J. Harvey, Negative ion mass spectrometry of sialylated carbohydrates: Discrimination of N-acetylneuraminic acid linkages by MALDI-TOF and ESI-TOF mass spectrometry, Anal. Chem. 72 (2000) 5027–5039.

[28]   C. Michael, A.M. Rizzi, Tandem mass spectrometry of isomeric aniline-labeled N-glycans separated on porous graphitic carbon: Revealing the attachment position of terminal sialic acids and structures of neutral glycans, Rapid Commun. Mass Spectrom. 29 (2015) 1268–1278.

[29]   D. Isailovic, R.T. Kurulugama, M.D. Plasencia, S.T. Stokes, Z. Kyselova, R. Goldman, Y. Mechref, M. V. Novotny, D.E. Clemmer, Profiling of Human Serum Glycans Associated with Liver Cancer and Cirrhosis by IMS−MS, J. Proteome Res. 7 (2008) 1109–1117.

[30]   M. Sarbu, F. Zhu, J. Peter-Katalinic, D.E. Clemmer, A.D. Zamfir, Application of ion mobility tandem mass spectrometry to compositional and structural analysis of glycopeptides extracted from the urine of a patient diagnosed with Schindler disease, Rapid Commun. Mass Spectrom. 29 (2015) 1929–1937.

[31]   M.M. Maurer, G.C. Donohoe, S.J. Valentine, Advances in ion mobility-mass spectrometry instrumentation and techniques for characterizing structural heterogeneity, Analyst. 140 (2015) 6782–6798.

24

561   [32] F. Lanucara, S.W. Holman, C.J. Gray, C.E. Eyers, The power of ion mobility-

562   mass spectrometry for structural characterization and the study of conformational

563   dynamics, Nat. Chem. 6 (2014) 281–294.

564   [33] D.M. Williams, T.L. Pukala, Novel insights into protein misfolding diseases

565   revealed by ion mobility-mass spectrometry, Mass Spectrom. Rev. 32 (2013)

566   169–187.

567   [34] B.T. Ruotolo, J.L.P. Benesch, A.M. Sandercock, S.-J. Hyung, C. V Robinson,

568   Ion mobility-mass spectrometry analysis of large protein complexes, Nat. Protoc.

569   3 (2008) 1139–1152.

570   [35] M.F. Bush, Z. Hall, K. Giles, J. Hoyes, C. V. Robinson, B.T. Ruotolo, Collision

571   cross sections of proteins and their complexes: A calibration framework and

572   database for gas-phase structural biology, Anal. Chem. 82 (2010) 9557–9565.

573   [36] A. Konijnenberg, J.F. van Dyck, L.L. Kailing, F. Sobott, Extending native mass

574   spectrometry approaches to integral membrane proteins, Biol. Chem. 396 (2015)

575   991–1002.

576   [37] Y. Sun, S. Vahidi, M.A. Sowole, L. Konermann, Protein Structural Studies by

577   Traveling Wave Ion Mobility Spectrometry: A Critical Look at Electrospray

578   Sources and Calibration Issues, J. Am. Soc. Mass Spectrom. 27 (2016) 31–40.

579   [38] A.B. Kanu, P. Dwivedi, M. Tam, L. Matz, H.H. Jr. Hill, Ion mobility–mass

580   spectrometry, J. Mass Spectrom. 43 (2008) 1–22.

581   [39] J.P. Williams, M. Kipping, J.P.C. Vissers, Traveling Wave Ion Mobility Mass

582   Spectrometry. Proteomic and Biopharmaceutical Applications, (n.d.) Waters.

583   Application Notes.

584   [40] A.A. Shvartsburg, R.D. Smith, Fundamentals of traveling wave ion mobility

585   spectrometry, Anal. Chem. 80 (2008) 9689–9699.

586   [41] D.J. Harvey, C.A. Scarff, M. Edgeworth, K. Pagel, K. Thalassinos, W.B. Struwe,

587   M. Crispin, J.H. Scrivens, Travelling-wave ion mobility mass spectrometry and

588   negative ion fragmentation of hybrid and complex N-glycans, J. Mass Spectrom.

589   51 (2016) 1064–1079.

590   [42] J. Hofmann, A. Stuckmann, M. Crispin, D.J. Harvey, K. Pagel, W.B. Struwe,

591   Identification of Lewis and Blood Group Carbohydrate Epitopes by Ion Mobility-

592   Tandem-Mass Spectrometry Fingerprinting, Anal. Chem. 89 (2017) 2318–2325.

593   [43] D.J. Harvey, C.A. Scarff, M. Edgeworth, W.B. Struwe, K. Pagel, K. Thalassinos,

M. Crispin, J. Scrivens, Travelling-wave ion mobility and negative ion fragmentation of high mannose N-glycans, J. Mass Spectrom. 51 (2016) 219–235.

[44] D. Bitto, D.J. Harvey, S. Halldorsson, K.J. Doores, L.K. Pritchard, J.T. Huiskonen, T.A. Bowden, M. Crispin, Determination of N -linked Glycosylation in Viral Glycoproteins by Negative Ion Mass Spectrometry and Ion Mobility, in: B. Lepenies (Ed.), Carbohydrate-Based Vaccines Methods Protoc., Springer New York, 2015: pp. 93–121.

[45] M. Guttman, K.K. Lee, Site-Specific Mapping of Sialic Acid Linkage Isomers by Ion Mobility Spectrometry, Anal. Chem. 88 (2016) 5212–5217.

[46] Y. Pu, M.E. Ridgeway, R.S. Glaskin, M.A. Park, C.E. Costello, C. Lin, Separation and Identification of Isomeric Glycans by Selected Accumulation-Trapped Ion Mobility Spectrometry-Electron Activated Dissociation Tandem Mass Spectrometry, Anal. Chem. 88 (2016) 3440–3443.

[47] X. Zheng, X. Zhang, N.S. Schocker, R.S. Renslow, D.J. Orton, J. Khamsi, R.A. Ashmus, I.C. Almeida, K. Tang, C.E. Costello, R.D. Smith, K. Michael, E.S. Baker, Enhancing glycan isomer separations with metal ions and positive and negative polarity ion mobility spectrometry-mass spectrometry analyses, Anal. Bioanal. Chem. 409 (2017) 467–476.

[48] J. Postigo, M. Iglesias, D. Cerezo-Wallis, A. Rosal-Vela, S. García-Rodríguez, M. Zubiaur, J. Sancho, R. Merino, J. Merino, Mice deficient in CD38 develop an attenuated form of collagen type II-induced arthritis, PLoS One. 7 (2012) e33534.

[49] J.J. Inglis, G. Criado, M. Medghalchi, M. Andrews, A. Sandison, M. Feldmann, R.O. Williams, Collagen-induced arthritis in C57BL/6 mice is associated with a robust and sustained T-cell response to type II collagen., Arthritis Res. Ther. 9 (2007) R113.

[50] A. Barroso, E. Giménez, F. Benavente, J. Barbosa, V. Sanz-Nebot, Analysis of human transferrin glycopeptides by capillary electrophoresis and capillary liquid chromatography-mass spectrometry. Application to diagnosis of alcohol dependence, Anal. Chim. Acta. 804 (2013) 167–175.

[51] A. Rosal-Vela, A. Barroso, E. Giménez, S. García-Rodríguez, V. Longobardo, J. Postigo, M. Iglesias, A. Lario, J. Merino, R. Merino, M. Zubiaur, V. Sanz-Nebot,

J. Sancho, Identification of multiple transferrin species in the spleen and serum from mice with collagen-induced arthritis which may reflect changes in transferrin glycosylation associated with disease activity: The role of CD38, J. Proteomics. 134 (2016) 127–137.

[52] C. Larriba, C.J. Hogan Jr., Free molecular collision cross section calculation methods for nanoparticles and complex ions with energy accommodation, J. Comput. Phys. 251 (2013) 344–363.

[53] C. Larriba, C.J. Hogan Jr., Ion mobilities in diatomic gases: Measurement versus prediction with non-specular scattering models, J. Phys. Chem. A. 117 (2013) 3887–3901.

[54] www.glycam.org. The University of Georgia. Complex Carbohydrate Research Center (CCRC), (n.d.).

[55] J. Marcoux, T. Champion, O. Colas, E. Wagner-Rousset, N. Corvaïa, A. Van Dorsselaer, A. Beck, S. Cianférani, Native mass spectrometry and ion mobility characterization of trastuzumab emtansine, a lysine-linked antibody drug conjugate, Protein Sci. 24 (2015) 1210–1223.

[56] D.J. Harvey, L. Royle, C.M. Radcliffe, P.M. Rudd, R.A. Dwek, Structural and quantitative analysis of N -linked glycans by matrix-assisted laser desorption ionization and negative ion nanospray mass spectrometry, Anal. Biochem. 376 (2008) 44–60.

[57] M. Mancera-Arteu, E. Giménez, J. Barbosa, R. Peracaula, V. Sanz-Nebot, Zwitterionic-hydrophilic interaction capillary liquid chromatography coupled to tandem mass spectrometry for the characterization of human alpha-acid-glycoprotein N-glycan isomers, Anal. Chim. Acta. In Press (2017).

[58] R.A. Feelders, G. Vreugdenhil, G. de Jong, A.J.G. Swaak, H.G. van Eijk, Transferrin microheterogeneity in rheumatoid arthritis. Relation with disease activity and anemia of chronic disease, Rheumatol. Int. 12 (1992) 195–199.

[59] Symbol Nomenclature for Graphical Representation of Glycans, Glycobiology. 25 (2015) 1323–1324.

Figure legends

659

660 **Figure 1**: Mass spectra showing the ion with charge +19 and the corresponding drift

661 time (arrival time) distributions, or ATD, of a) intact mTf and b) intact hTf; and also c)

662 ions with charge +13, +12 and +11 of intact hAGP and the corresponding ATD. The

663 value indicated corresponds to the approximate glycosylation percentage (w/w) of each

664 protein, calculated as the mass of the most abundant glycan per glycosylation site

665 divided by the mass of the glycoprotein. i)-v): indicates the glycoform or the region of

666 the mass spectrometric peak. H: hexose; N: N-acetylhexosamine; F: fucose; S: sialic

667 acid (in this case, all S are N-glycolylneuraminic acid). The voltages for spray capillary,

668 sampling cone, trap collision energy (CE), trap direct current (DC) bias and transfer CE

669 were, respectively: 1.4-1.6 kV, 30 V, 4 V, 40 V and 0 V.

670

671 **Figure 2**: a) MS/MS spectrum for the mTf glycopeptide glycoform

672 N(H5N4S2)STLCDLCIGPLK; b) mass spectra of a fragment that still keeps the sialic

673 acid (H1N1S1) and c) arrival time distribution of this fragment (m/z range: 673.3-

674 673.5). The symbols used for the representation of the glycoform H5N4S2 follow the

675 Symbol Nomenclature for Glycans (SNFG) rules [59]. H: hexose; N: N-

676 acetylhexosamine; F: fucose; S: sialic acid (in this case, all S are N-glycolylneuraminic

677 acid). The voltages for spray capillary, sampling cone, trap collision energy (CE), trap

678 direct current (DC) bias and transfer CE were, respectively: 1.5-1.7 kV, 50 V, 4 V, 20 V

679 and 60 V.

680

681 **Figure 3**: Arrival time distributions for the H5N4S2 glycan released from mTf at

682 different wave height (WH, in V) and wave velocity (WV, in m s^{-1}) combinations. The

683 symbols used for the representation of the H5N4S2 glycan follow the Symbol

684 Nomenclature for Glycans (SNFG) rules [59]. H: hexose; N: N-acetylhexosamine; F:

685 fucose; S: sialic acid (in this case, all S are N-glycolylneuraminic acid). The voltages for

686 spray capillary, sampling cone, trap collision energy (CE), trap direct current (DC) bias

687 and transfer CE were, respectively: 1.5 kV, 50 V, 4 V, 45 V and 0 V.

688

689 **Figure 4**: Arrival time distributions for the glycans a) H5N4S2 and b) H6N5S3 released

690 from mTf in a healthy mouse serum and a serum from a mouse with collagen-induced

691 arthritis (CIA). The symbols used for the glycan representation follow the Symbol

692 Nomenclature for Glycans (SNFG) rules [59]. H: hexose; N: N-acetylhexosamine; F:

693 fucose; S: sialic acid (in this case, all S are N-glycolylneuraminic acid). The voltages for

694 spray capillary, sampling cone, trap collision energy (CE), trap direct current (DC) bias

695 and transfer CE were, respectively: 1.5 kV, 50 V, 4 V, 45 V and 0 V.

1

Evaluation of Iion mobility for the separation of glycoconjugate isomers due to

different types of sialic acid linkage, at the intact glycoprotein, glycopeptide and

glycan level

Albert Barroso[1], Estela Giménez[1,†], Albert Konijnenberg[2], Jaime Sancho[3], Victoria Sanz-Nebot[1], Frank Sobott[2,4,5,‡]

[1] Department of Chemical Engineering and Analytical Chemistry, University of Barcelona, Diagonal 645, 08028 Barcelona, Spain

[2] Biomolecular & Analytical Mass Spectrometry group, Department of Chemistry, University of Antwerp, Antwerp, Belgium

[3] Instituto de Parasitología y Biomedicina "López-Neyra" (IPBLN), CSIC, Armilla, Granada, Spain

[4] Astbury Centre for Structural Molecular Biology, University of Leeds, Leeds LS2 9JT, United Kingdom

[5] School of Molecular and Cellular Biology, University of Leeds, LS2 9JT, United Kingdom

Corresponding author: [†]Tel.: +34 934021278; fax: +34 934021233; e-mail address: estelagimenez@ub.edu;

[‡]F. Sobott: e-mail address: frank.sobott@leeds.ac.ukuantwerpen.be

Abbreviations: ATD: arrival time distribution; CCS: collision cross section; CIA: collagen-induced arthritis; hAGP: human α-1-acid glycoprotein; hTf: human transferrin; IM-MS: ion mobility – mass spectrometry; mTf: mouse transferrin; nano-ESI: nano electrospray ionization; nano-UPLC: nano ultra performance liquid chromatography; TOF: time-of-flight; TWIMS: travelling wave ion mobility spectrometry.

KEYWORDS: glycosylation, ion mobility, isomers, mouse transferrin, sialic acid.

24   **ABSTRACT**

25   The study of protein glycosylation can be regarded as an intricate but very important

26   task, making glycomics one of the most challenging and interesting, albeit under-

27   researched, type of "omics" science. Complexity escalates remarkably when

28   considering that carbohydrates can form severely branched structures with many

29   different constituents, which often leads to the formation of multiple isomers. In this

30   regard, ion mobility (IM) spectrometry has recently demonstrated its power for the

31   separation of isomeric compounds. In the present work, the potential of traveling wave

32   IM (TWIMS) for the separation of isomeric glycoconjugates was evaluated, using

33   mouse transferrin (mTf) as model glycoprotein. Particularly, we aim to assess the

34   performance of this platform for the separation of isomeric glycoconjugates due to the

35   type of sialic acid linkage, at the intact glycoprotein, glycopeptide and glycan level.

36   Straightforward separation of isomers was achieved with the analysis of released

37   glycans, as opposed to the glycopeptides which showed a more complex pattern.

38   Finally, the developed methodology was applied to serum samples of mice, to

39   investigate its robustness when analysing real complex samples.

40

41

1. Introduction

Glycosylation is by far one of the most common and complex posttranslational modifications, with more than half of all secretory and cellular proteins being glycosylated [1–3]. Carbohydrates enhance the functional diversity of proteins, but they can also define their destination or elicit an immune response. The presence of glycans in the surface of eukaryotic cells is vital, as they take part in important cellular events, such as cell–cell interactions and receptor recognition [4]. Notwithstanding its importance and the major role of glycosylation in a multitude of biological processes [5–7], the analysis and characterization of carbohydrates is usually difficult due to their inherent complexity - the main reason why advances in glycomics have been scarcer compared to other "omics" sciences [8,9]. Very often, in contrast to more linearly assembled biological molecules such as proteins or oligonucleotides, carbohydrates can form complex structures, severely branched, with many monosaccharide constituents, which usually results in a multitude of isomers [10].

Mass spectrometry (MS)-based techniques are the prime option for the characterization of glycoproteins, as reliable structural information can be obtained [7,11]. MS is frequently used in conjunction with chromatographic or electrophoretic separation techniques, as this allows high sensitivity profiling and accurate characterisation of heterogeneous glycan structures [12–14]. However, when analysing isomeric glycan structures, MS often fails to separate them [8,15–17], as they have identical mass and atomic composition. Some authors have suggested alternative strategies to separate isomeric glycoconjugates based on their derivatization, —or the use of capillary electrophoresis (CE) or hydrophilic interaction liquid chromatography (HILIC)— thus they remain undistinguishable unless derivatization or less common stationary phases in

3

66 ~~liquid chromatography (LC) are used~~ [18–23]. But even then, derivatization protocols

67 can be time-consuming, expensive or hinder the ionization of some glycans, or, in the

68 case of ~~LC~~CE or HILIC, the unambiguous identification is still impossible when

69 different isomers coelute. Moreover, in the last few years, several tandem mass

70 spectrometry (MS/MS) methods have been reported that allow the identification of

71 glycan isomers and the characterization of their structure [24–26]. However, few

72 authors have studied the fragmentation of glycans with different sialic acid linkages.

73 Even then, distinguishing by MS/MS between isomeric glycans due to sialic acid

74 linkage is not trivial and, quite often, is based on differences in the relative abundance

75 of certain fragment ions [27,28]. Therefore, a straightforward technique that helps to

76 separate and differentiate those isomeric compounds is much needed.

77 In this regard, ion-mobility (IM) spectrometry coupled with MS has aroused some

78 interest in the last years, not only in the glycomics field but also in other omics sciences,

79 as a proficient analytical technique for the separation of isomeric compounds

80 [3,8,10,15–17,29–31]. Ion mobility provides an additional dimension for the separation

81 of compounds, where ions are not only separated due to their mass and charge, but also

82 on the basis of their shape and size - thereby resolving ions that would be otherwise

83 indistinguishable solely by MS, such as, for instance, isomers [32–36]. Particularly, IM

84 measures the time (drift time) that a particular ion takes to cross a cell filled with an

85 inert, neutral background gas (N_2 and He are most commonly used) at a controlled

86 pressure under the influence of a weak electric field. The drift time of a specific ion is

87 mainly due to ion-gas collisions; therefore, ions are separated due to their ion-neutral

88 collision cross-section (Ω), related to the overall shape and topology of the ion [32–36].

89 Small compact ions have the shortest drift times, i.e. they arrive first, as a result of their

4

90   smaller Ω. Moreover, the higher the charge of the ion, the greater the accelerating

91   electric force, and therefore the more quickly the ion will cross the chamber.

92   Consequently, the drift time of an ion is often described as being determined by the

93   collision cross-section-to-charge ratio (Ω/z) [35]. When coupled on-line with MS (IM-

94   MS), ion mobility provides three-dimensional analytical information for each detected

95   species, i.e. shape-to-charge, mass-to-charge and abundance, thus allowing reliable

96   analyte identification.

97   Nowadays, there are several IM methods next to the classical drift-time ion mobility

98   spectrometry (DTIMS), such as field asymmetric waveform ion mobility spectrometry

99   (FAIMS), but among them, traveling wave ion mobility spectrometry (TWIMS) is the

100   one that has seen a major growth in the last years [37,38]. In TWIMS, ions are propelled

101   thanks to a sequence of symmetric potential waves continually propagating through a

102   cell, each ion with its own velocity, thus different species transit the cell in different

103   times. One of the main advantages of TWIMS is that it disperses ion mixtures, allowing

104   the simultaneous measurement of multiple species. This, in conjunction with a high

105   sensitivity obtained when TWIMS is coupled to certain analyzers in MS, such as time-

106   of-flight (TOF), has made this platform an alluring option for structural analysis and

107   isomer separation [38–40]. This platform, along with other IM methods, have been

108   recently explored for the analysis of glycans or glycoconjugates by several authors

109   [8,15,16,41–47].

110   In this work, TWIMS combined with TOF-MS was used for the study of

111   glycoconjugate isomers which differ in the type of sialic acid linkage, with mouse

112   transferrin (mTf) as a model glycoprotein. Sialic acid, an important monosaccharide

113   residue of complex type N-glycans, may form primarily two types of linkages: α-2→-3

114   or α-2→-6. We aim to assess the capacity of TWIMS-TOF-MS (from now on referred

115   to as IM-MS) as an analytical platform to separate α-2→-3 and α-2→-6 isomeric

116   glycoconjugates at the intact glycoprotein, glycopeptide and glycan level. The

117   developed methodology was also applied to serum samples of mice, to confirm its

118   robustness when analysing real complex samples.

119

2. Materials and methods

2.1 Chemicals

All chemicals used in the preparation of buffers and solutions were of analytical reagent grade. Isopropanol (iPrOH), hydrochloric acid (HCl, 37% (w/v)), formic acid (FA, 98–100%), ammonium acetate (NH$_4$Ac, ≥98.0%) and glycine (≥99.7%) were supplied by Merck (Darmstadt, Germany). CNBr-activated-Sepharose 4B was provided by GE Healthcare (Waukesha, WI, USA) and "NP-40 alternative" by Calbiochem (Darmstadt, Germany). Sodium chloride (NaCl, ≥99.5%), DL-Dithiothreitol (DTT, ≥99%), sodium cyanoborohydride (NaBH$_3$CN), 2-mercaptoethanol (β-ME), sodium dodecyl sulfate (SDS), iodoacetamide (IAA), ammonium hydrogencarbonate, sodium azide (NaN$_3$, ≥99.5%) water (LC-MS grade), acetonitrile (LC–MS grade) and mouse apotransferrin (mTf, reference: T0523) were supplied by Sigma–Aldrich (St. Louis, MO, USA) and Tris(hydroxymethyl) aminomethane (TRIS, ≥99.5%) by J.T. Baker (Deventer, Holland). Trypsin (Sequencing grade modified) was provided by Promega (Madison, WI, USA). RapiGest® from Waters (Bedford, MA, USA) was used to facilitate the enzymatic digestion. Goat polyclonal antibody against human transferrin (hTf) (immunogen affinity purified) was purchased from Abcam (Cambridge, UK). Human transferrin (hTf) and human α-1-acid glycoprotein (hAGP) were used as additional examples of other glycosylated glycoproteins and were also supplied by Sigma–Aldrich.

2.2 Mice and induction of arthritis

Wild-type (WT) mice were from Harlan Ibérica (Barcelona, Spain). All studies with live animals were authorized by the Institute of Parasitology and Biomedicine "López-Neyra" (IPBLN) and Universidad de Cantabria Institutional Laboratory Animal Care

143 and Use Committees. For the induction of collagen-induced arthritis (CIA), 8-12 weeks-

144 old male mice were immunized as described elsewhere [48,49].

145 **2.3 Purification of serotransferrin from mouse serum samples by immunoaffinity**

146 **chromatography (IAC)**

147 In order to isolate mTf from the rest of serum proteins, an immunoaffinity (IA)

148 purification was carried out using a cyanogen-bromide sepharose column where a

149 polyclonal antibody against human transferrin (hTf) was bound, as detailed previously

150 [50]. The IA procedure consisted of: first, a conditioning step with two washes of 10

151 mM Tris-HCl; second, approximately 25 µL of serum were diluted 1:8 in 10 mM Tris-

152 HCl (pH 7.6-7.7) in order to improve antigen-antibody interaction, and passed through

153 the column ten times. After washing with 10 mM Tris-HCl and 0.5 M NaCl (pH 7.6-

154 7.7), retained mTf was eluted with 100 mM glycine-HCl (pH 2.5). Eluted mTf was

155 immediately neutralized with 0.5 M Tris. Afterwards, glycine-HCl buffer was

156 exchanged for water by ultracentrifugation, using Microcon YM-10 (MW cut-off 10

157 kDa, Millipore, Bedford, MA, USA). Then, samples were evaporated to dryness using a

158 SpeedVac^{TM} concentrator (Thermo Fisher Scientific, Waltham, MA, USA) and stored at

159 -20ºC until use. Finally, the IA column was washed and stored in 10 mM Tris-HCl and

160 0.01% (w/v) NaN$_3$ (pH 7.6-7.7).

161 **2.4 Analytical approaches for mTf glycosylation study**

162 2.4.1 <u>Intact glycoprotein analysis</u>

163 mTf standard (25 µg) was desalted using three different procedures: dialysis, size

164 exclusion and ultracentrifugation. Briefly, in the first method, D-Tube^{TM} dialyzers from

165 Merck-Millipore were left in contact with 100 mM NH$_4$Ac for 15 min. Afterwards, the

8

166 sample was placed into the dialyzer and left in contact with 500 mL of 100 mM NH$_4$Ac

167 for 2 h at 4ºC. Later, the buffer was renewed with 500 mL and the dialysis was allowed

168 to continue for 2 more hours, repeating this process twice. Finally, the sample was

169 carefully recovered and stored at -20ºC until analysis. Regarding the size exclusion

170 procedure, the sample was desalted and the buffer exchanged using Micro Bio-Spin^{TM}

171 columns from BioRad (Hercules, California, USA) following the manufacturer

172 instructions. Columns were centrifuged to remove the excess of packing buffer and

173 washed three times with 500 μL of 100 mM NH$_4$Ac. Finally, the sample was added and

174 collected in a new tube after centrifugation. Lastly, the ultracentrifugation procedure

175 was carried out using Microcon YM-10 (MW cut-off 10 kDa) to desalt and exchange

176 the buffer of the sample. Filters were washed with 100 mM NH$_4$Ac and centrifuged for

177 10 min at 10000 g. Afterwards, the sample was added and washed with 50 μL of 100

178 mM NH$_4$Ac a total of 4 times, centrifuging each time for 10 min at 10000 g. Finally, the

179 final volume was recovered in a new vial after centrifugation for 2 min at 1000 g, and

180 reconstituted to the initial volume (25 μL). Centrifugation procedures were carried out

181 in a MiniSpin$^®$ centrifuge (Eppendorf, Hamburg, Germany) at room temperature. In all

182 cases, experiments with the standard glycoprotein were carried out in triplicate and

183 intact mTf in 100 mM NH$_4$Ac was injected directly into the mass spectrometer under

184 non-denaturing conditions and detected in positive ion mode.

185 2.4.2   Glycopeptide analysis

186 mTf standard (25 μg) w~~as~~as reduced, alkylated and immediately subjected to trypsin

187 digestion in the presence of RapiGest$^®$ as explained in ~~a~~ previous work [51]. Briefly, a

188 solution of 0.5 M DL-dithiothreitol (DTT) in 50 mM NH$_4$HCO$_3$ was added to an aliquot

189 of mTf with 0.1% (w/v) RapiGest$^®$. The mixture was incubated at 56ºC for 30 min and

9

then alkylated with 50 mM iodoacetamide (IAA) for 30 min at room temperature in the dark. Excess reagent was removed by ultracentrifugation with Microcon YM-10 columns (Millipore, Bedford, MA, USA). The final residue was recovered from the upper reservoir and reconstituted with NH_4HCO_3 buffer with 0.1% RapiGest®. Trypsin in a 1:40 ratio was added and the mixture was incubated overnight at 37ºC. Afterwards, the surfactant was hydrolyzed to avoid MS incompatibilities as follows: formic acid (FA) was added to the digest to a final concentration of 5% (v/v) and the mixture was incubated in the digester at 37ºC for 30 min. Then, the solution was centrifuged to separate RapiGest® residues. mTf tryptic digests were stored at -20ºC until analysis. All the experiments with the standard glycoprotein were carried out in triplicate.

For the analysis of glycopeptides, a Waters Nano ACQUITY UPLC® was used with a double binary gradient pump, using a peptide BEH C18 column (1.7 µm particle diameter, 130 Å pore, 100 x 0.1 mm length x ID; Waters). Experiments were performed at room temperature with gradient elution at a flow rate of 400 nL min^{-1}. Eluting solvents were A: water with 0.1% (v/v) of formic acid (FA), and B: acetonitrile with 0.1% (v/v) FA. Solvents were degassed by sonication (10 min) before use. The optimum elution program was: solvent B from 10 to 60% (v/v) within 20 min as linear gradient, followed by cleaning and re-equilibration steps of B: 60 to 100% (v/v) (5 min), 100% (v/v) (5 min), 100 to 10% (v/v) (5 min) and 10% (v/v) (5 min). Before analysis, samples were filtered using a 0.22 µm polyvinylidene difluoride centrifugal filter (Ultrafree-MC, Millipore, Bedford, MA, USA) centrifuging at 10,000 g for 4 min. Sample injection (300 nL) was performed with an autosampler refrigerated at 4ºC. Control of the instrument was performed using MassLynx 4.1 (Waters).

2.4.3   Glycan analysis

214 ~~IAC purified mTf or mTf standard (25 μg) was reduced with 0.5% 2-mercaptoethanol~~

215 ~~(β-ME) and 0.5% SDS and subjected to enzymatic digestion with PNGase F as~~

216 ~~described in.~~IAC purified mTf or mTf standard (25 μg) was reduced with 0.5% 2-

217 mercaptoethanol (β-ME) and 0.5% SDS in 50 mM NH_4HCO_3 (pH 7.6-7.7) and heated

218 in a thermo -block at 100 °C for 30 min [19]. Once the sample was at room temperature,

219 a volume of 50 mM NH_4HCO_3 (pH 7.6-7.7) with 1% (v/v) of NP-40 alternative was

220 added to obtain a final concentration of 0.1% SDS and β-ME in the sample. To release

221 the N-glycans, 1μL of PNGase F (1 U) solution was added to the mixture, which was

222 afterwards incubated at 37°C for 18 h. Digestion was stopped by heating the sample in a

223 thermo block at 100°C for 5 min. ~~Afterwards~~Then, released glycans were isolated by

224 solid phase extraction (SPE) using Hypercarb cartridges (25 mg, 1 mL volume, Thermo

225 Fisher Scientific) and, subsequently, purified by ice-cold acetone precipitation

226 following the procedure reported in [19] in both cases. Reduced glycans were diluted

227 with 50:50 H_2O/ACN with 0.1% FA and directly analyzed by IM-MS in negative ion

228 mode. All the experiments with the standard glycoprotein were carried out in triplicate.

229 Mice derived transferrin glycan analysis was carried out in duplicate, including

230 purification and release of glycans.

231 **2.5 Ion mobility-mass spectrometry**

232 For IM-MS analysis a Synapt G2 HDMS instrument from Waters was used. Samples

233 were directly introduced into the ~~vacuum of the~~ mass spectrometer using home-made

234 nano-electrospray ionization (nano-ESI) gold-coated borosilicate capillaries;~~,~~ unless

235 when analysed by nano-UPLC-IM-MS, in which case an in-line nano-ESI interface with

236 commercially available coated needles was used.

237 Spectra were acquired in positive mode for the analysis of intact glycoproteins and

238 glycopeptides, and in negative mode for glycans, and conditions were optimized in each

239 case. The voltages for spray capillary, sampling cone, trap collision energy (CE), trap

240 direct current (DC) bias and transfer CE were, respectively: intact glycoproteins, 1.4-1.6

241 kV, 30 V, 4 V, 40 V and 0 V; glycopeptides, 1.5-1.7 kV, 50 V, 4 V, 20 V and 0 V; and

242 glycans, 1.5 kV, 50 V, 4 V, 45 V and 0 V. The "trap CE" voltage was only increased to

243 60 V when fragmentation of the glycopeptides was the goal. Mass spectrometer control

244 and spectra processing were carried out using MassLynx 4.1 (Waters).

245 The software IMoS [52,53], available for free at imospedia.com, was used for the

246 theoretical calculations of the collision cross sections (CCS) of glycans, using their

247 minimum energy structures. The online tool carbohydrate builder, available at

248 glycam.org [54], was used to generate the required input for theoretical calculations.

249 The tool allows building different glycan isomers based on monosaccharide unit and

250 linkage type, and generates minimum energy structures.

251

3. Results and discussion

3.1   Intact glycoprotein analysis

It is well established that intact proteins can be analysed mainly in two different ways when using electrospray ionization: under denaturing or non-denaturing (i.e., "native") conditions. In the first case, the protein appears highly charged with a broad charge state distribution; thus, the separation of the different glycoforms is difficult. On the other hand, an advantage of native MS is that it strongly reduces charging, hence the different glycoforms can be more clearly resolved [55].

Using native MS in this work, the concentration of ammonium acetate and the nano-ESI source parameters were optimized to improve and obtain the best possible sensitivity and separation between mTf glycoforms in positive ion mode. Moreover, in order to obtain an acceptable separation between the several glycoforms, mTf was washed repeatedly with 100 mM NH_4Ac to eliminate excipients and salts, and injected directly into the mass spectrometer without further separation. Without washing, no glycoform separation was observed whatsoever. Three methods were evaluated to desalt the glycoprotein: dialysis, size exclusion and ultracentrifugation, with the latter one giving the best results (see supplementary Figure S1). Afterwards, the drift times of intact glycoforms were determined by ion mobility. In Figure 1-a, the ion with charge +19 of mTf is shown, as well as the arrival time distributions (ATD) of different sections of this peak (Figure 1-a (i-v)), each corresponding to one intact glycoform of mTf). As can be observed in the ATD profiles, only one, relatively wide peak is obtained for each glycoform. Hence, these results imply that, at least for large glycoproteins with a low degree of glycosylation, the glycan part has barely any influence on the overall size of the whole molecule as the CCS appears virtually unaffected by glycosylation. hTf and

13

276   hAGP were also studied to see if the same behaviour was observed with other

277   glycoproteins. Figure 1-b and 1-c show the separation between intact glycoforms in the

278   MS spectra of hTf (for the ion with charge +19) and hAGP, respectively. As can be

279   observed, the peak was better resolved for hTf, but no separation was observed for

280   hAGP, as the number of glycoforms was considerably higher and the overlapping of

281   several ion distributions was unavoidable. Moreover, one wide peak was observed again

282   when the drift time of each section of the mass spectrum was measured for both

283   glycoproteins. Regarding hTf, each section corresponded to one glycoform (Figure 1-b

284   (i-iv)), whereas, in the case of hAGP, the resolution was not high enough to ensure that

285   a selected region of the peak corresponded to one defined glycoform (Figure 1-c (i-v)),

286   because of the high glycosylation degree of hAGP. The higher the m/z region of this

287   peak however, the bigger the carbohydrate fraction is (usually meaning more complex

288   and branched glycans). This is due to the fact that an increase of m/z within the same

289   charge state can only be due to an increase in the number of glycan subunits of the

290   carbohydrate fraction, as the polypeptide backbone remains unaltered. For the sake of

291   consistency, we will refer to each section of the peak as glycoform, even if, as in the

292   case of hAGP, they are not resolved. Interestingly, the drift time increased with

293   increasing carbohydrate fraction, i.e. complexity and branching of the glycoforms, in all

294   three cases (see Figure 1-a (i-v), 1-b (i-iv) and 1-c (i-v), type of glycoform indicated

295   where possible). The relative drift time differences between glycoforms were higher in

296   proteins with higher glycosylation content, as can be observed for hAGP (see Figure 1-

297   c). Moreover, if we compare the drift time between different glycoforms of mTf and

298   hTf, the increase in drift time was more noticeable in hTf, as the percentage of

299   glycosylation is slightly higher here in relation to the total protein mass. As Table 1

300   shows, for the same relative increase in m/z, the relative drift time increase is higher for

14

301　hAGP, which demonstrates that for glycoproteins with a high percentage of

302　glycosylation, differences in the glycosylation have a greater effect on the drift time of

303　the whole molecule (i.e., they significantly alter the CCS of the whole glycoprotein). It

304　could then also be conceivable to separate isomers due to the different sialic acid

305　linkage (of the same glycoform) at the intact protein level if the glycan:peptide ratio was

306　high enough. However, this option would not have been viable for all types of

307　glycoproteins, thus, other alternatives were studied.

3.2 Glycopeptide analysis

309　As mTf only shows one glycosite at asparagine 494, only one glycopeptide is expected

310　after tryptic digestion (N_{494} glycopeptide, peptide: NSTLCDLCIGPLK). However, with

311　the direct injection of the digest, the N_{494} glycopeptide was not detected, hence, an

312　additional separation before the MS was mandatory. In this regard, nano-UPLC was

313　used as a separation technique prior to IM-MS detection, in order to separate the

314　glycopeptide from the other peptides and simultaneously determine the drift time of the

315　different glycoforms. Injection volume, flow rate and gradient were optimized to obtain

316　the best sensitivity with a stable spray (see section 2.4, Materials and Methods). Table 2

317　shows the detected glycoforms at the peptide level, their theoretical and experimental

318　masses, mass error and observed charge states.

319　Regarding the determination of the drift time of the different glycopeptide glycoforms,

320　even though a range of different values for the wave velocity (WV) and wave height

321　(WH) of the TWIMS device were tested, only one drift time value was observed. This

322　suggests that no isomer separation was possible at this mobility resolution, which is

323　probably due to the fact that the different isomers had similar CCS despite the distinct

324　orientation of the sialic acid. Recently, Hinneburg et al. [15] and Guttman et al. [45]

15

325   also described this observation analysing glycopeptides directly by IM-MS. They

326   observed no isomeric separation, unless fragmentation of the glycopeptide was carried

327   out and one of the observed smaller fragments still contained the sialic acid. This

328   fragment (obtained before the IM cell) had different drift times depending on the sialic

329   acid linkage, because a change in the orientation of the sialic acid was more noticeable

330   (i.e. the CCS was more affected) in a smaller analyte. We also tested this approach, by

331   fragmenting the most intense glycopeptide glycoform (N(H5N4S2)STLCDLCIGPLK)

332   before the IM cell. Figure 2-a shows the collision induced dissociation (CID) MS/MS

333   spectrum for this glycoform. Several fragments were obtained, e.g., the

334   glycolylneuraminic acid (S1) and H1N1 and H2N1 fragments. Among all the fragments

335   however, H1N1S1 was the one that still retained the sialic acid linkage and had enough

336   intensity to yield a good and accurate drift time measurement. Isomer separation was

337   observed in the aforementioned glycan fragment. Specifically, as it is shown in Figure

338   2-c, two drift time peaks were clearly observed at this m/z, which are postulated to be

339   due to the sialic acid being α-2-$\rightarrow$6 and α-2$\rightarrow$-3 linked. To confirm that the sialic acid is

340   the monosaccharide that affects the CCS of the fragment the most, the ATD of the

341   fragment H1N1 is shown in supplementary Figure S2-c. In this case, we only observed

342   one drift time, which demonstrates that it is the sialic acid which causes observable CCS

343   differences seen as two different drift times of the fragment H1N1S1.

344   Moreover, in order to confirm that the distinct drift times observed for the glycan

345   fragment could be due to different sialic acid linkages, the theoretical CCS of the

346   H1N1S1 isomers were calculated. The obtained CCS values can be found in Table 3.

347   were: 233.4 Å² for the α-2→6 linkage and 243.7 Å² for the α-2→3 glycan, The CCS for

348   the two H1N1S1 were different enough to be separated by IM. Taking into account the

349 CCS values of Table 3, ~~This suggests that~~ the more prominent, lower drift time peak

350 (i.e., lower CCS) should corresponds to the α~~-2→~~-6 glycan, whereas the second peak

351 represents the α~~-2→~~-3 glycan.

352 Our results are in accordance with those obtained by Hinneburg et al. [15], who, using

353 modelling, drew the same conclusions. This is also in agreement with Guttman et al.

354 [45], who found that biantennary glycoforms showed lower content of α-2→-3

355 sialylation. In our case, the percentage of α-2--→3 glycan was approximately 14%

356 (taking into account the measured area of each drift time peak, see Figure 2-c).

357 However, this ratio can vary depending on the glycoprotein studied [45]. ~~With this~~

358 ~~method, using nano-UPLC-IM-MS and drift time measurement of the MS/MS~~

359 ~~fragments, separation of glycopeptide isomers was achieved.~~This glycopeptide

360 approach, through the analysis of the fragment H1N1S1, gave valuable information

361 about the content of each type of sialic acid as the fragment H1N1S1 came from both

362 branches of the H5N4S2 glycopeptide (we did not detect any fragment with only one

363 antenna remaining (H3N3 or H3N3S1), suggesting that both antennas might indeed be

364 fragmented). This relevant information could permit, in the future, to correlate changes

365 in protein sialylation with specific disease biomarkers which involve protein

366 glycosylation, such as, e.g., in cancer or inflammation.

367

368 **3.3 Glycan analysis**

369 Finally, we proceeded with the study of the enzymatically released glycans using

370 PNGase F. Different solvents were tested to obtain the best spray and ionization yield,

371 and a slightly superior glycan signal was obtained at 50:50 H_2O:ACN with 0.1% FA.

372   Table ~~3~~ 4 shows the detected mTf glycans along with their theoretical and experimental

373 masses, mass error and observed charge states. In Figure 3 the ATD profile of H5N4S2

374 glycans at different values of WV and WH is shown. Two peaks are observed which are

375 believed to correspond to two different isomers of the glycan H5N4S2, in analogy to the

376 previously obtained results (Figure 2-c) with the fragment H1N1S1 of the glycopeptide

377 N(H5N4S2)STLCDLCIGPLK. Fine tuning of the IM parameters was mandatory in

378 order to resolve both drift time peaks. A WV value of 450 m s^{-1} and WH of 25 V was

379 selected as optimal for the analysis of all mTf glycans. It is worth mentioning that in

380 this case, glycans were analyzed in negative mode and, as can be observed in Figure 3,

381 the first isomer was clearly the less abundant one. This is in contrast to the glycopeptide

382 analysis which was done in positive mode, where the less abundant isomer was the

383 second one. This could be due to the fact that both molecules were, actually, quite

384 different - specifically, the glycan had eleven monosaccharide units, as opposed to the

385 fragment observed in the glycopeptide analysis which had only three. With regard to

386 other glycans, three different peaks, i.e., three drift times, were observed for H6N5S3

387 (see supplementary Figure ~~2~~S3-c), albeit separation was slightly worse than observed

388 for H5N4S2. H5N4S1 on the other hand only showed one wide peak (see

389 supplementary Figure ~~2~~S3-d), ~~most probably~~ implying that only one glycan isomer

390 exists or that the different isomers have similar CCS, and IM is not able to distinguish

391 them (as~~. However,~~ the absence of other drift time peaks does not preclude the presence

392 of other isomers)~~., as they can have similar CCS.~~ It is also worth pointing out that when

393 the glycan contained a fucose unit, the isomeric separation was somewhat hampered, as

394 observed in supplementary Figure ~~2~~S3-b. We reckon that the addition of one extra

395 monosaccharide unit might affect the global CCS of the glycan, and as the whole glycan

396 is bigger, a small variation in the orientation of the sialic acid is less noticeable.

397   To confirm that separation of isomeric glycans due to the sialic acid linkage was also

398   possible with other glycoproteins, hAGP was also digested with PNGase F and the

399   released glycans analysed by IM-MS. Separation of isomeric glycans was achieved,

400   seemingly obtaining the same results as with mTf. As an example, the arrival time

401   distributions of the H5N4S2 and H6N5S2 glycans are shown in supplementary Figure

402   ~~3~~S4. As can be seen, two drift time peaks were obtained for the H5N4S2 glycan and

403   three peaks for H6N5S3, albeit separation was poorer in both cases when compared to

404   mTf.

405   Moreover, to confirm that ion mobility separation of these possible isomers is due to

406   different sialic acid linkages, Table 3 shows the theoretical CCS values of the four

407   possible isomers for the glycan H5N4S2 ~~with (α-2 →3)$_2$, (α-2 →6) and (α-2 →3), (α-26)~~

408   ~~nd (α-2 →3) and (α-2 →6)$_2$ sialic acids were calculated. The obtained CCS were,~~

409   ~~following the same order: 652.3 Å^2 for the (α-2 →3)$_2$ glycan, 635.4 Å^2 for (α-2 →6)(α-~~

410   ~~2 →3),~~ xxx Å^2 ~~and 623.9 Å^2 for the (α-2 →6)$_2$ form~~. The differences between these

411   calculated values suggest that the observed ion mobility peaks could be due to isomeric

412   glycans with different types of sialic acid linkage. With the knowledge of theoretical

413   CCS, and the abundance of the α-2-→3 H1N1S1 fragment being lower than ~~the~~ α-2→-6

414   (based on fragmentation of the H5N4S2 glycopeptide, see above), ~~the two peaks~~

415   ~~observed for the H5N4S2 glycan were tentatively assigned~~some conclusions can be

416   drawn. We reckon that the presence of the isomer with two sialic acids α2-3 can be

417   discarded and that the two peaks observed must correspond to the isomers with higher

418   content in α2-6, that is, the isomer with two sialic acids α2-6 and the isomer with one

419   sialic acid α2-6 and one α2-3 (although we cannot specify the branch where each sialic

420   acid is located).~~We suggest that the peak with the highest drift time, and highest~~

421 ~~abundance, could be the glycan (α-2→6)(α-2→3) linkage~~, however, we cannot specify

422 the branch where each sialic acid is ~~located~~bound. ~~Whereas, the one with the lowest~~

423 ~~drift time (and lowest abundance) could be the (α-2→6)₂-linked glycan.~~ However,

424 <u>A</u>~~a~~lternative approaches for the study of isomeric glycoconjugates, for instance using

425 specific sialidases [18], ~~could~~ <u>would however</u> ~~be~~ <u>allow to</u> ~~useful to~~ obtain

426 complementary information and reliably assign the different ~~isomers~~<u>peaks to the</u>

427 <u>corresponding isomers</u>.

428 **3.4 M<u>ous</u>~~ic~~e serum sample**

429 To further asses the ability of the established method to separate isomeric

430 glycoconjugates in biological samples, we measured the drift time of mTf glycans

431 purified from serum samples. Only the analysis of the released glycans by IM-MS was

432 included in this study, as it was found to be the most sensitive and straightforward

433 approach to obtain information about isomeric forms. Two serum samples were

434 analysed: one healthy control and one sample with collagen-induced arthritis (CIA), an

435 autoimmune disease known to alter the glycosylation pattern of mTf [51,58]. As can be

436 seen in Figure 4, two peaks were observed for H5N4S2 glycan and three peaks for

437 H6N5S3 in both samples, with the same drift time and similar relative intensities as in

438 the mTf standard (compare Figure 4 with supplementary Figure ~~2~~<u>S3</u>). Although

439 additional samples are required to observe possible differences in the relative abundance

440 of glycan isomers between control and pathological samples, the presented

441 methodology shows great potential for the separation of isomeric glycans and the

442 discovery of novel biomarkers in glycomic studies.

443

4. Concluding remarks

In the present paper, the capability of IM-MS to separate isomeric glycoconjugates which are due to different types of sialic acid linkage (i.e. α-2→-3 and α-2→-6) has been evaluated at three different levels: intact glycoprotein, glycopeptides, and the released glycans. Separation of isomeric glycoconjugates is an important task in the glycomics field, because it has been reported that differences in the abundance of some glycan isomers might be of great importance for the early diagnosis or control of, for instance, inflammatory diseases and certain types of cancer.

With ~~our~~the current knowledge of glycosylation effects on molecule size, and the limited ability~~capabilities~~ of Synapt IM-MS instrumentation to resolve small CCS differences, isomeric separation cannot be obtained at the intact glycoprotein and glycopeptide level. Released glycans however can be separated after optimization of the IM parameters. As stated before by others [15,45], and also demonstrated in this work, there is a workaround to distinguish different types of sialic acid linkage in glycopeptides that takes into account the mobility of an MS/MS fragment which still retains the sialic acid. This method can however be time-consuming and rather difficult, as glycopeptides must be separated from the rest of the digest and, besides, the obtained glycopeptide fragment is, actually, a glycan.

The interest in using ion mobility for glycoconjugate separation and identification has seen a major growth in the last years. Thus, it is likely that new technologies and improvements will become available soon, including the advent of ion mobility instrumentation with up to ten times higher resolution. Therefore, the separation of sialic acid linkage isomers may also become possible at the level of glycopeptides and intact proteins in the future.

468

469

Acknowledgements

476

5. References

[1] A.P. Corfield, M. Berry, Glycan variation and evolution in the eukaryotes, Trends Biochem. Sci. 40 (2015) 351–359.

[2] H.A. Abbass, H.A. El Hassan, H. Bahmad, A. Zebian, R. Youssef, J. Ismail, R. Zhu, S. Zhou, X. Dong, M. Nasser, M. Bahmad, H. Darwish, Y. Mechref, F. Kobeissy, Glycosylation and other post translational modifications alterations in neurodegenerative diseases: current status and future role in neurotrauma, Electrophoresis. 37 (2016) 1549–1561.

[3] F. Zhu, J.C. Trinidad, D.E. Clemmer, Glycopeptide Site Heterogeneity and Structural Diversity Determined by Combined Lectin Affinity Chromatography/IMS/CID/MS Techniques, J. Am. Soc. Mass Spectrom. 26 (2015) 1092–1102.

[4] A. Grigorian, S. Torossian, M. Demetriou, T-cell growth, cell surface organization, and the galectin glycoprotein lattice, Immunol. Rev. 230 (2009) 232–246.

[5] R.A. Dwek, Glycobiology: towards understanding the function of sugars, Chem. Rev. 96 (1996) 683–720.

[6] P.M. Rudd, T. Elliott, P. Cresswell, I.A. Wilson, R.A. Dwek, Glycosylation and the immune system, Science (80-.). 291 (2001) 2370–2376.

[7] H.J. Allen, E.C. Kisailus, eds., Glycoconjugates: Composition: Structure, and Function, CRC Press, 1992.

[8] J. Hofmann, H.S. Hahm, P.H. Seeberger, K. Pagel, Identification of carbohydrate anomers using ion mobility-mass spectrometry, Nature. 526 (2015) 241–244.

[9] K. Mariño, J. Bones, J.J. Kattla, P.M. Rudd, A systematic approach to protein glycosylation analysis: a path through the maze, Nat. Chem. Biol. 6 (2010) 713–723.

[10] K. Pagel, D.J. Harvey, Ion Mobility − Mass Spectrometry of Complex Carbohydrates: Collision Cross Sections of Sodiated N-linked Glycans, Anal. Chem. 85 (2013) 5138–5145.

[11] N. Leymarie, J. Zaia, Effective use of mass spectrometry for glycan and glycopeptide structural analysis, Anal. Chem. 84 (2012) 3040–3048.

[12] M.L.M. Hennrich, A.A. Gavin, Quantitative mass spectrometry of posttranslational modifications: Keys to confidence, Sci. Signal. 8 (2015) 1–5.

511   [13]   M. Wuhrer, Glycomics using mass spectrometry, Glycoconj. J. 30 (2013) 11–22.

512   [14]   Y. Zhang, J. Jiao, P. Yang, H. Lu, Mass spectrometry-based N-glycoproteomics

513   for cancer biomarker discovery, Clin. Proteomics. 11 (2014) 18.

514   [15]   H. Hinneburg, J. Hofmann, W.B. Struwe, A. Thader, F. Altmann, D. Varón Silva,

515   P.H. Seeberger, K. Pagel, D. Kolarich, Distinguishing N-acetylneuraminic acid

516   linkage isomers on glycopeptides by ion mobility-mass spectrometry, Chem.

517   Commun. 52 (2016) 4381–4384.

518   [16]   D.J. Harvey, C.A. Scarff, M. Edgeworth, M. Crispin, C.N. Scanlan, F. Sobott, S.

519   Allman, K. Baruah, L. Pritchard, J.H. Scrivens, Travelling wave ion mobility and

520   negative ion fragmentation for the structural determination of N-linked glycans,

521   Electrophoresis. 34 (2013) 2368–2378.

522   [17]   P. Both, A.P. Green, C.J. Gray, R. Šardzík, J. Voglmeir, C. Fontana, M. Austeri,

523   M. Rejzek, D. Richardson, R.A. Field, G. Widmalm, S.L. Flitsch, C.E. Eyers,

524   Discrimination of epimeric glycans and glycopeptides using IM-MS and its

525   potential for carbohydrate sequencing, Nat Chem. 6 (2014) 65–74.

526   [18]   M. Mancera-Arteu, E. Giménez, J. Barbosa, V. Sanz-Nebot, Identification and

527   characterization of isomeric N-glycans of human alfa-acid-glycoprotein by stable

528   isotope labelling and ZIC-HILIC-MS in combination with exoglycosidase

529   digestion, Anal. Chim. Acta. 940 (2016) 92–103.

530   [19]   E. Giménez, M. Balmaña, J. Figueras, E. Fort, C. Bolós, V. Sanz-Nebot, R.

531   Peracaula, A. Rizzi, Quantitative analysis of N-glycans from human alfa-acid-

532   glycoprotein using stable isotope labeling and zwitterionic hydrophilic

533   interaction capillary liquid chromatography electrospray mass spectrometry as

534   tool for pancreatic disease diagnosis, Anal. Chim. Acta. 866 (2015) 59–68.

535   [20]   R.B. Parker, J.E. McCombs, J.J. Kohler, Sialidase specificity determined by

536   chemoselective modification of complex sialylated glycans, ACS Chem. Biol. 7

537   (2012) 1509–1514.

538   [21]   P. Jackson, M.I. Attalla, N-Nitrosopiperazines form at high pH in post-

539   combustion capture solutions containing piperazine: a low-energy collisional

540   behaviour study, Rapid Commun. Mass Spectrom. 24 (2010) 3567–3577.

541   [22]   F. Tousi, J. Bones, W.S. Hancock, M. Hincapie, Differential chemical

542   derivatization integrated with chromatographic separation for analysis of

543   isomeric   sialylated   N-glycans: a   nano-hydrophilic   interaction   liquid

544   chromatography-MS platform, Anal. Chem. 85 (2013) 8421–8428.

545 [23] G.S.M. Kammeijer, B.C. Jansen, I. Kohler, A.A.M. Heemskerk, O.A.
546   Mayboroda, P.J. Hensbergen, J. Schappler, M. Wuhrer, Sialic acid linkage
547   differentiation of glycopeptides using capillary electrophoresis – electrospray
548   ionization – mass spectrometry, Sci. Rep. 7 (2017) 3733.

549 [24] A. V. Everest-Dass, J.L. Abrahams, D. Kolarich, N.H. Packer, M.P. Campbell,
550   Structural feature ions for distinguishing N- and O-linked glycan isomers by LC-
551   ESI-IT MS/MS, J. Am. Soc. Mass Spectrom. 24 (2013) 895–906.

552 [25] E. V. Da Costa, A.S.P. Moreira, F.M. Nunes, M.A. Coimbra, D. V. Evtuguin,
553   M.R.M. Domingues, Differentiation of isomeric pentose disaccharides by
554   electrospray ionization tandem mass spectrometry and discriminant analysis,
555   Rapid Commun. Mass Spectrom. 26 (2012) 2897–2904.

556 [26] S. Zhou, X. Dong, L. Veillon, Y. Huang, Y. Mechref, LC-MS/MS analysis of
557   permethylated N-glycans facilitating isomeric characterization, Anal. Bioanal.
558   Chem. 409 (2017) 453–466.

559 [27] S.F. Wheeler, D.J. Harvey, Negative ion mass spectrometry of sialylated
560   carbohydrates: Discrimination of N-acetylneuraminic acid linkages by MALDI-
561   TOF and ESI-TOF mass spectrometry, Anal. Chem. 72 (2000) 5027–5039.

562 [28] C. Michael, A.M. Rizzi, Tandem mass spectrometry of isomeric aniline-labeled
563   N-glycans separated on porous graphitic carbon: Revealing the attachment
564   position of terminal sialic acids and structures of neutral glycans, Rapid
565   Commun. Mass Spectrom. 29 (2015) 1268–1278.

566 [29] D. Isailovic, R.T. Kurulugama, M.D. Plasencia, S.T. Stokes, Z. Kyselova, R.
567   Goldman, Y. Mechref, M. V. Novotny, D.E. Clemmer, Profiling of Human
568   Serum Glycans Associated with Liver Cancer and Cirrhosis by IMS–MS, J.
569   Proteome Res. 7 (2008) 1109–1117.

570 [30] M. Sarbu, F. Zhu, J. Peter-Katalinic, D.E. Clemmer, A.D. Zamfir, Application of
571   ion mobility tandem mass spectrometry to compositional and structural analysis
572   of glycopeptides extracted from the urine of a patient diagnosed with Schindler
573   disease, Rapid Commun. Mass Spectrom. 29 (2015) 1929–1937.

574 [31] M.M. Maurer, G.C. Donohoe, S.J. Valentine, Advances in ion mobility-mass
575   spectrometry instrumentation and techniques for characterizing structural
576   heterogeneity, Analyst. 140 (2015) 6782–6798.

577   [32] F. Lanucara, S.W. Holman, C.J. Gray, C.E. Eyers, The power of ion mobility-
578   mass spectrometry for structural characterization and the study of conformational
579   dynamics, Nat. Chem. 6 (2014) 281–294.

580   [33] D.M. Williams, T.L. Pukala, Novel insights into protein misfolding diseases
581   revealed by ion mobility-mass spectrometry, Mass Spectrom. Rev. 32 (2013)
582   169–187.

583   [34] B.T. Ruotolo, J.L.P. Benesch, A.M. Sandercock, S.-J. Hyung, C. V Robinson,
584   Ion mobility-mass spectrometry analysis of large protein complexes, Nat. Protoc.
585   3 (2008) 1139–1152.

586   [35] M.F. Bush, Z. Hall, K. Giles, J. Hoyes, C. V. Robinson, B.T. Ruotolo, Collision
587   cross sections of proteins and their complexes: A calibration framework and
588   database for gas-phase structural biology, Anal. Chem. 82 (2010) 9557–9565.

589   [36] A. Konijnenberg, J.F. van Dyck, L.L. Kailing, F. Sobott, Extending native mass
590   spectrometry approaches to integral membrane proteins, Biol. Chem. 396 (2015)
591   991–1002.

592   [37] Y. Sun, S. Vahidi, M.A. Sowole, L. Konermann, Protein Structural Studies by
593   Traveling Wave Ion Mobility Spectrometry: A Critical Look at Electrospray
594   Sources and Calibration Issues, J. Am. Soc. Mass Spectrom. 27 (2016) 31–40.

595   [38] A.B. Kanu, P. Dwivedi, M. Tam, L. Matz, H.H. Jr. Hill, Ion mobility–mass
596   spectrometry, J. Mass Spectrom. 43 (2008) 1–22.

597   [39] J.P. Williams, M. Kipping, J.P.C. Vissers, Traveling Wave Ion Mobility Mass
598   Spectrometry. Proteomic and Biopharmaceutical Applications, (n.d.) Waters.
599   Application Notes.

600   [40] A.A. Shvartsburg, R.D. Smith, Fundamentals of traveling wave ion mobility
601   spectrometry, Anal. Chem. 80 (2008) 9689–9699.

602   [41] D.J. Harvey, C.A. Scarff, M. Edgeworth, K. Pagel, K. Thalassinos, W.B. Struwe,
603   M. Crispin, J.H. Scrivens, Travelling-wave ion mobility mass spectrometry and
604   negative ion fragmentation of hybrid and complex N-glycans, J. Mass Spectrom.
605   51 (2016) 1064–1079.

606   [42] J. Hofmann, A. Stuckmann, M. Crispin, D.J. Harvey, K. Pagel, W.B. Struwe,
607   Identification of Lewis and Blood Group Carbohydrate Epitopes by Ion Mobility-
608   Tandem-Mass Spectrometry Fingerprinting, Anal. Chem. 89 (2017) 2318–2325.

609   [43] D.J. Harvey, C.A. Scarff, M. Edgeworth, W.B. Struwe, K. Pagel, K. Thalassinos,

610 M. Crispin, J. Scrivens, Travelling-wave ion mobility and negative ion
611 fragmentation of high mannose N-glycans, J. Mass Spectrom. 51 (2016) 219–
612 235.

613 [44] D. Bitto, D.J. Harvey, S. Halldorsson, K.J. Doores, L.K. Pritchard, J.T.
614 Huiskonen, T.A. Bowden, M. Crispin, Determination of N -linked Glycosylation
615 in Viral Glycoproteins by Negative Ion Mass Spectrometry and Ion Mobility, in:
616 B. Lepenies (Ed.), Carbohydrate-Based Vaccines Methods Protoc., Springer New
617 York, 2015: pp. 93–121.

618 [45] M. Guttman, K.K. Lee, Site-Specific Mapping of Sialic Acid Linkage Isomers by
619 Ion Mobility Spectrometry, Anal. Chem. 88 (2016) 5212–5217.

620 [46] Y. Pu, M.E. Ridgeway, R.S. Glaskin, M.A. Park, C.E. Costello, C. Lin,
621 Separation and Identification of Isomeric Glycans by Selected Accumulation-
622 Trapped Ion Mobility Spectrometry-Electron Activated Dissociation Tandem
623 Mass Spectrometry, Anal. Chem. 88 (2016) 3440–3443.

624 [47] X. Zheng, X. Zhang, N.S. Schocker, R.S. Renslow, D.J. Orton, J. Khamsi, R.A.
625 Ashmus, I.C. Almeida, K. Tang, C.E. Costello, R.D. Smith, K. Michael, E.S.
626 Baker, Enhancing glycan isomer separations with metal ions and positive and
627 negative polarity ion mobility spectrometry-mass spectrometry analyses, Anal.
628 Bioanal. Chem. 409 (2017) 467–476.

629 [48] J. Postigo, M. Iglesias, D. Cerezo-Wallis, A. Rosal-Vela, S. García-Rodríguez,
630 M. Zubiaur, J. Sancho, R. Merino, J. Merino, Mice deficient in CD38 develop an
631 attenuated form of collagen type II-induced arthritis, PLoS One. 7 (2012)
632 e33534.

633 [49] J.J. Inglis, G. Criado, M. Medghalchi, M. Andrews, A. Sandison, M. Feldmann,
634 R.O. Williams, Collagen-induced arthritis in C57BL/6 mice is associated with a
635 robust and sustained T-cell response to type II collagen., Arthritis Res. Ther. 9
636 (2007) R113.

637 [50] A. Barroso, E. Giménez, F. Benavente, J. Barbosa, V. Sanz-Nebot, Analysis of
638 human transferrin glycopeptides by capillary electrophoresis and capillary liquid
639 chromatography-mass spectrometry. Application to diagnosis of alcohol
640 dependence, Anal. Chim. Acta. 804 (2013) 167–175.

641 [51] A. Rosal-Vela, A. Barroso, E. Giménez, S. García-Rodríguez, V. Longobardo, J.
642 Postigo, M. Iglesias, A. Lario, J. Merino, R. Merino, M. Zubiaur, V. Sanz-Nebot,

J. Sancho, Identification of multiple transferrin species in the spleen and serum from mice with collagen-induced arthritis which may reflect changes in transferrin glycosylation associated with disease activity: The role of CD38, J. Proteomics. 134 (2016) 127–137.

[52] C. Larriba, C.J. Hogan Jr., Free molecular collision cross section calculation methods for nanoparticles and complex ions with energy accommodation, J. Comput. Phys. 251 (2013) 344–363.

[53] C. Larriba, C.J. Hogan Jr., Ion mobilities in diatomic gases: Measurement versus prediction with non-specular scattering models, J. Phys. Chem. A. 117 (2013) 3887–3901.

[54] www.glycam.org. The University of Georgia. Complex Carbohydrate Research Center (CCRC), (n.d.).

[55] J. Marcoux, T. Champion, O. Colas, E. Wagner-Rousset, N. Corvaïa, A. Van Dorsselaer, A. Beck, S. Cianférani, Native mass spectrometry and ion mobility characterization of trastuzumab emtansine, a lysine-linked antibody drug conjugate, Protein Sci. 24 (2015) 1210–1223.

[56] D.J. Harvey, L. Royle, C.M. Radcliffe, P.M. Rudd, R.A. Dwek, Structural and quantitative analysis of N -linked glycans by matrix-assisted laser desorption ionization and negative ion nanospray mass spectrometry, Anal. Biochem. 376 (2008) 44–60.

[57] M. Mancera-Arteu, E. Giménez, J. Barbosa, R. Peracaula, V. Sanz-Nebot, Zwitterionic-hydrophilic interaction capillary liquid chromatography coupled to tandem mass spectrometry for the characterization of human alpha-acid-glycoprotein N-glycan isomers, Anal. Chim. Acta. In Press (2017).

[58] R.A. Feelders, G. Vreugdenhil, G. de Jong, A.J.G. Swaak, H.G. van Eijk, Transferrin microheterogeneity in rheumatoid arthritis. Relation with disease activity and anemia of chronic disease, Rheumatol. Int. 12 (1992) 195–199.

[59] Symbol Nomenclature for Graphical Representation of Glycans, Glycobiology. 25 (2015) 1323–1324.

674 **Figure legends**

675

676 **Figure 1**: Mass spectra showing the ion with charge +19 and the corresponding drift

677 time (arrival time) distributions, or ATD, of a) intact mTf and b) intact hTf; and also c)

678 ions with charge +13, +12 and +11 of intact hAGP and the corresponding ATD. The

679 value indicated corresponds to the approximate glycosylation percentage (w/w) of each

680 protein, calculated as the mass of the most abundant glycan per glycosylation site

681 divided by the mass of the glycoprotein. i)-v): indicates the glycoform or the region of

682 the mass spectrometric peak. H: hexose; N: N-acetylhexosamine; F: fucose; S: sialic

683 acid (in this case, all S are N-glycolylneuraminic acid). The voltages for spray capillary,

684 sampling cone, trap collision energy (CE), trap direct current (DC) bias and transfer CE

685 were, respectively: 1.4-1.6 kV, 30 V, 4 V, 40 V and 0 V.

686 **Figure 2**: a) MS/MS spectrum for the mTf glycopeptide glycoform

687 N(H5N4S2)STLCDLCIGPLK; b) mass spectra of a fragment that still keeps the sialic

688 acid (H1N1S1) and c) arrival time distribution of this fragment (m/z range: 673.3-

689 673.5). The symbols used for the representation of the glycoform H5N4S2 follow the

690 ~~Consortium for Functional Glycomics~~Symbol Nomenclature for Glycans (SNFG)

691 ~~(CFG)~~ rules [59]. H: hexose; N: N-acetylhexosamine; F: fucose; S: sialic acid (in this

692 case, all S are N-glycolylneuraminic acid). The voltages for spray capillary, sampling

693 cone, trap collision energy (CE), trap direct current (DC) bias and transfer CE were,

694 respectively: 1.5-1.7 kV, 50 V, 4 V, 20 V and 60 V.

695 **Figure 3**: Arrival time distributions for the H5N4S2 glycan released from mTf at

696 different wave height (WH, in V) and wave velocity (WV, in m s^{-1}) combinations. The

697 symbols used for the representation of the H5N4S2 glycan follow the Symbol

698 Nomenclature for Glycans (SNFG) ~~Consortium for Functional Glycomics (CFG)~~ rules

699   [59]. H: hexose; N: N-acetylhexosamine; F: fucose; S: sialic acid (in this case, all S are

700   N-glycolylneuraminic acid). The voltages for spray capillary, sampling cone, trap

701   collision energy (CE), trap direct current (DC) bias and transfer CE were, respectively:

702   1.5 kV, 50 V, 4 V, 45 V and 0 V.

703   **Figure 4**: Arrival time distributions for the glycans a) H5N4S2 and b) H6N5S3 released

704   from mTf in a healthy mouse serum and a serum from a mouse with collagen-induced

705   arthritis (CIA). The symbols used for the glycan representation follow the Symbol

706   Nomenclature for Glycans (SNFG) ~~Consortium for Functional Glycomics (CFG)~~ rules

707   [59]. H: hexose; N: N-acetylhexosamine; F: fucose; S: sialic acid (in this case, all S are

708   N-glycolylneuraminic acid). The voltages for spray capillary, sampling cone, trap

709   collision energy (CE), trap direct current (DC) bias and transfer CE were, respectively:

710   1.5 kV, 50 V, 4 V, 45 V and 0 V.

711

712   **Figure S1**: Mass spectra of the ion with charge +19 of intact mTf after desalting with

713   three different methods: a) dialysis, b) size exclusion columns, and c)

714   ultracentrifugation. The voltages for spray capillary, sampling cone, trap collision

715   energy (CE), trap direct current (DC) bias and transfer CE were, respectively: 1.4-1.6

716   kV, 30 V, 4 V, 40 V and 0 V.

717   **Figure S2:** a) MS/MS spectrum for the mTf glycopeptide glycoform

718   N(H5N4S2)STLCDLCIGPLK; b) mass spectra of a fragment that still keeps the sialic

719   acid (H1N1) and c) arrival time distribution of this fragment (m/z range: 366.2-366.4).

720   The symbols used for the representation of the glycoform H5N4S2 follow the Symbol

721   Nomenclature for Glycans (SNFG) rules [59]. H: hexose; N: N-acetylhexosamine; F:

722 fucose; S: sialic acid (in this case, all S are N-glycolylneuraminic acid). The voltages for

723 spray capillary, sampling cone, trap collision energy (CE), trap direct current (DC) bias

724 and transfer CE were, respectively: 1.5-1.7 kV, 50 V, 4 V, 20 V and 60 V.

725

726 **Figure 2S3**: Arrival time distributions for several glycans of mTf standard: a) H5N4S2,

727 b) H5N4F1S2, c) H6N5S3 and d) H5N4S1. The symbols used for the glycan

728 representation follow the Symbol Nomenclature for Glycans (SNFG) Consortium for

729 Functional Glycomics (CFG) rules [59]. H: hexose; N: N-acetylhexosamine; F: fucose;

730 S: sialic acid (in this case, all S are N-glycolylneuraminic acid). The voltages for spray

731 capillary, sampling cone, trap collision energy (CE), trap direct current (DC) bias and

732 transfer CE were, respectively: 1.5 kV, 50 V, 4 V, 45 V and 0 V.

733

734 **Figure 3S4:** Arrival time distributions for a) H5N4S2 glycan and b) H6N5S3 glycan of

735 hAGP. The symbols used for the glycan representation follow the Symbol

736 Nomenclature for Glycans (SNFG) rules [59]Consortium for Functional Glycomics

737 (CFG) rules. H: hexose; N: N-acetylhexosamine; F: fucose; S: sialic acid (in this case,

738 all S are N-acetylneuraminic acid). The voltages for spray capillary, sampling cone, trap

739 collision energy (CE), trap direct current (DC) bias and transfer CE were, respectively:

740 1.5 kV, 50 V, 4 V, 45 V and 0 V.

741

742

743   **Table 1:** Relative increase in m/z and drift time between glycoforms i) and ii) (Figure

744   1) of mTf, hTf and hAGP.

		mTf	hTf	hAGP
Relative m/z difference (%)		0.247	0.239	0.746
Relative drift time difference (%)		0.149	0.290	1.324
Normalization*	**Relative m/z (%)**	0.247	0.247	0.247
	Relative drift time (%)	0.149	0.299	0.438

745

746   ***** The relative m/z for hTf and hAGP was changed to have the same value as mTf

747   (0.247 %) and, therefore, the relative drift time was proportionally modified.

748

749

750 **Table 2:** Theoretical and experimental molecular mass (Mr), mass error and detected

751 charge states of the 10 glycoforms for the N_{494} glycopeptide of mTf detected by nano-

752 UPLC-IM-MS.

753

Glycopeptide	Glycoform*	Theoretical M_r	Experimental M_r	Mass error (ppm)	Observed charge state
N_{494}	H3N3S1	2892.2138	2892.2840	24	+2
	H3N3F1S1	3038.2717	3038.2920	7	+2
	H5N4S1	3419.3988	3419.3908	2	+2, +3
	H5N4F1S1	3565.4568	3565.4656	2	+3
	H5N4S2	3726.4892	3726.4993	3	+2, +3
	H5N4F1S2	3872.5471	3872.5600	3	+2, +3
	H5N4S3	4033.579	4033.6210	10	+2, +3
	H5N4F1S3	4179.6374	4179.6958	14	+2, +3
	H6N5S3	4398.7117	4398.7813	16	+3
	H6N5F1S3	4544.7696	4544.8321	14	+3

754 * H: hexose; N: N-acetylhexosamine; F: fucose; S: sialic acid (in this case, all S are N-

755 glycolylneuraminic acid)

756

757 **Table 3:** CCS values of the two isomers for the fragment H1N1S1 and the four isomers

758 for the H5N4S2 glycan.

			Isomer	CCS (Å^2)
Glycopeptide N$_{494}$-H5N4S2	Fragment	H1N1S1	α2-6	233.4
		H1N1S1	α2-3	243.7
Glycan H5N4S2			3-antenna α2-6 6-antenna α2-3	584.7
			2 x α2-6	623.9
			3-antenna α2-3 6-antenna α2-6	635.4
			2 x α2-3	652.3

759

760   **Table ~~3~~4:** Theoretical and experimental molecular mass (Mr), mass error and detected

761   charge states of the 10 mTf glycans detected by IM-MS.

Glycan*	Theoretical M_r	Experimental M_r	Mass error (ppm)	Observed charge state
H3N3S1	1420.4975	1420.4659	22	-1
H3N3F1S1	1566.5554	1566.5692	9	-1
H5N4S1	1947.6825	1947.7031	11	-1
H5N4F1S1	2093.7404	2093.7891	23	-1
H5N4S2	2254.7729	2254.7650	4	-2
H5N4F1S2	2400.8308	2400.8240	3	-2
H5N4S3	2561.8632	2561.9150	20	-2
H5N4F1S3	2707.9211	2707.9470	10	-2
H6N5S3	2926.9954	2926.9334	21	-2, -3
H6N5F1S3	3073.0533	3073.0036	16	-3

762

763

764   * H: hexose; N: N-acetylhexosamine; F: fucose; S: sialic acid (in this case, all S are N-

765   glycolylneuraminic acid)

766

767

768

769

770

Table 1: Relative increase in m/z and drift time between glycoforms i) and ii) (Figure

1) of mTf, hTf and hAGP.

		mTf	hTf	hAGP
Relative m/z difference (%)		0.247	0.239	0.746
Relative drift time difference (%)		0.149	0.290	1.324
Normalization*	Relative m/z (%)	0.247	0.247	0.247
	Relative drift time (%)	0.149	0.299	0.438

* The relative m/z for hTf and hAGP was changed to have the same value as mTf

(0.247 %) and, therefore, the relative drift time was proportionally modified.

Table 2: Theoretical and experimental molecular mass (Mr), mass error and detected charge states of the 10 glycoforms for the N_{494} glycopeptide of mTf detected by nano-UPLC-IM-MS.

Glycopeptide	Glycoform*	Theoretical M_r	Experimental M_r	Mass error (ppm)	Observed charge state
N_{494}	H3N3S1	2892.2138	2892.2840	24	+2
	H3N3F1S1	3038.2717	3038.2920	7	+2
	H5N4S1	3419.3988	3419.3908	2	+2, +3
	H5N4F1S1	3565.4568	3565.4656	2	+3
	H5N4S2	3726.4892	3726.4993	3	+2, +3
	H5N4F1S2	3872.5471	3872.5600	3	+2, +3
	H5N4S3	4033.579	4033.6210	10	+2, +3
	H5N4F1S3	4179.6374	4179.6958	14	+2, +3
	H6N5S3	4398.7117	4398.7813	16	+3
	H6N5F1S3	4544.7696	4544.8321	14	+3

* H: hexose; N: N-acetylhexosamine; F: fucose; S: sialic acid (in this case, all S are N-glycolylneuraminic acid)

Table 3: CCS values of the two isomers for the fragment H1N1S1 and the four isomers

for the H5N4S2 glycan.

			Isomer	CCS (Å^2)
Glycopeptide N$_{494}$-H5N4S2	Fragment	H1N1S1	α2-6	233.4
		H1N1S1	α2-3	243.7
Glycan H5N4S2			3-antenna α2-6 6-antenna α2-3	584.7
			2 x α2-6	623.9
			3-antenna α2-3 6-antenna α2-6	635.4
			2 x α2-3	652.3

Table 4: Theoretical and experimental molecular mass (Mr), mass error and detected charge states of the 10 mTf glycans detected by IM-MS.

Glycan*	Theoretical M_r	Experimental M_r	Mass error (ppm)	Observed charge state
H3N3S1	1420.4975	1420.4659	22	-1
H3N3F1S1	1566.5554	1566.5692	9	-1
H5N4S1	1947.6825	1947.7031	11	-1
H5N4F1S1	2093.7404	2093.7891	23	-1
H5N4S2	2254.7729	2254.7650	4	-2
H5N4F1S2	2400.8308	2400.8240	3	-2
H5N4S3	2561.8632	2561.9150	20	-2
H5N4F1S3	2707.9211	2707.9470	10	-2
H6N5S3	2926.9954	2926.9334	21	-2, -3
H6N5F1S3	3073.0533	3073.0036	16	-3

* H: hexose; N: N-acetylhexosamine; F: fucose; S: sialic acid (in this case, all S are N-glycolylneuraminic acid)
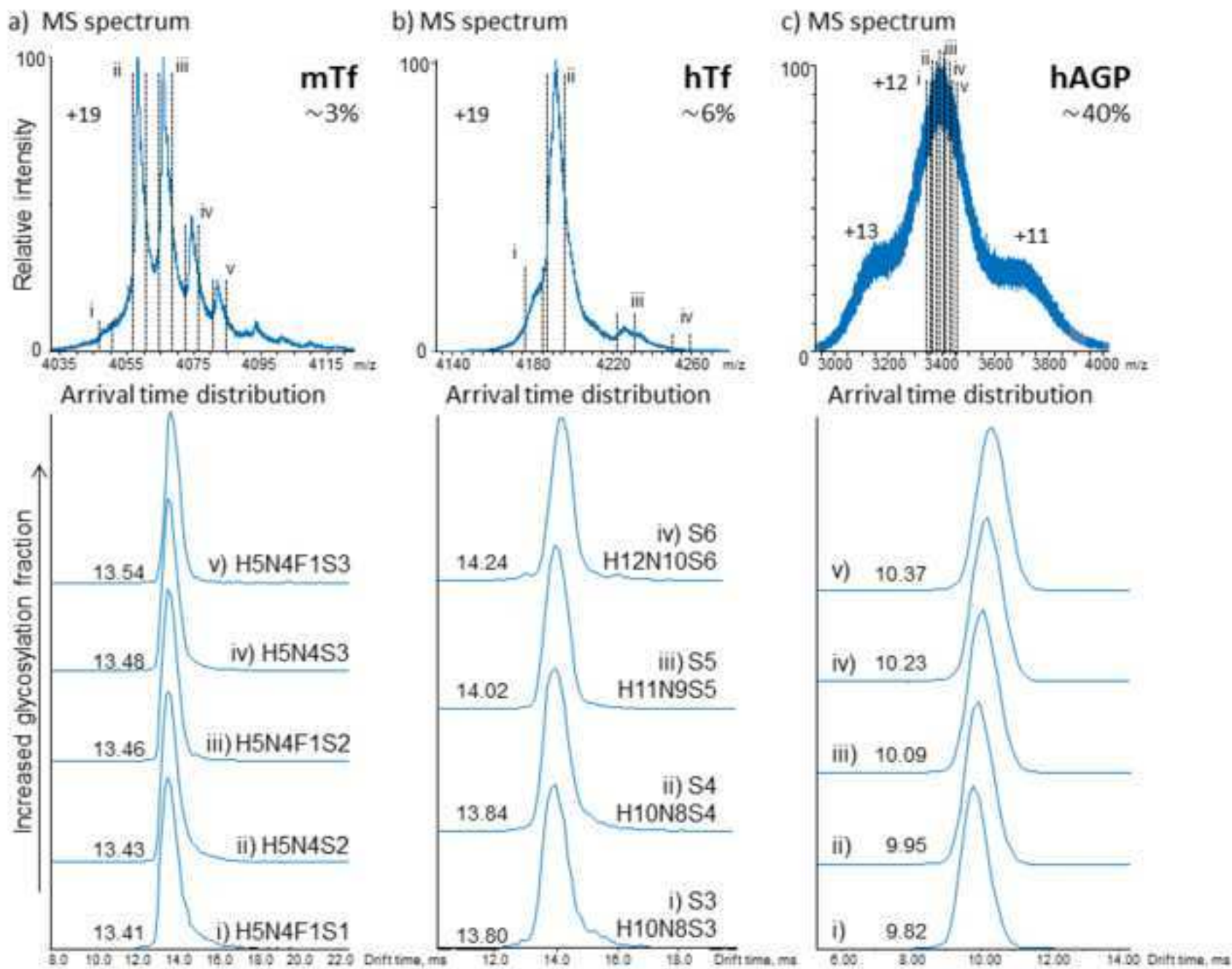
Figure 1

Figure 2
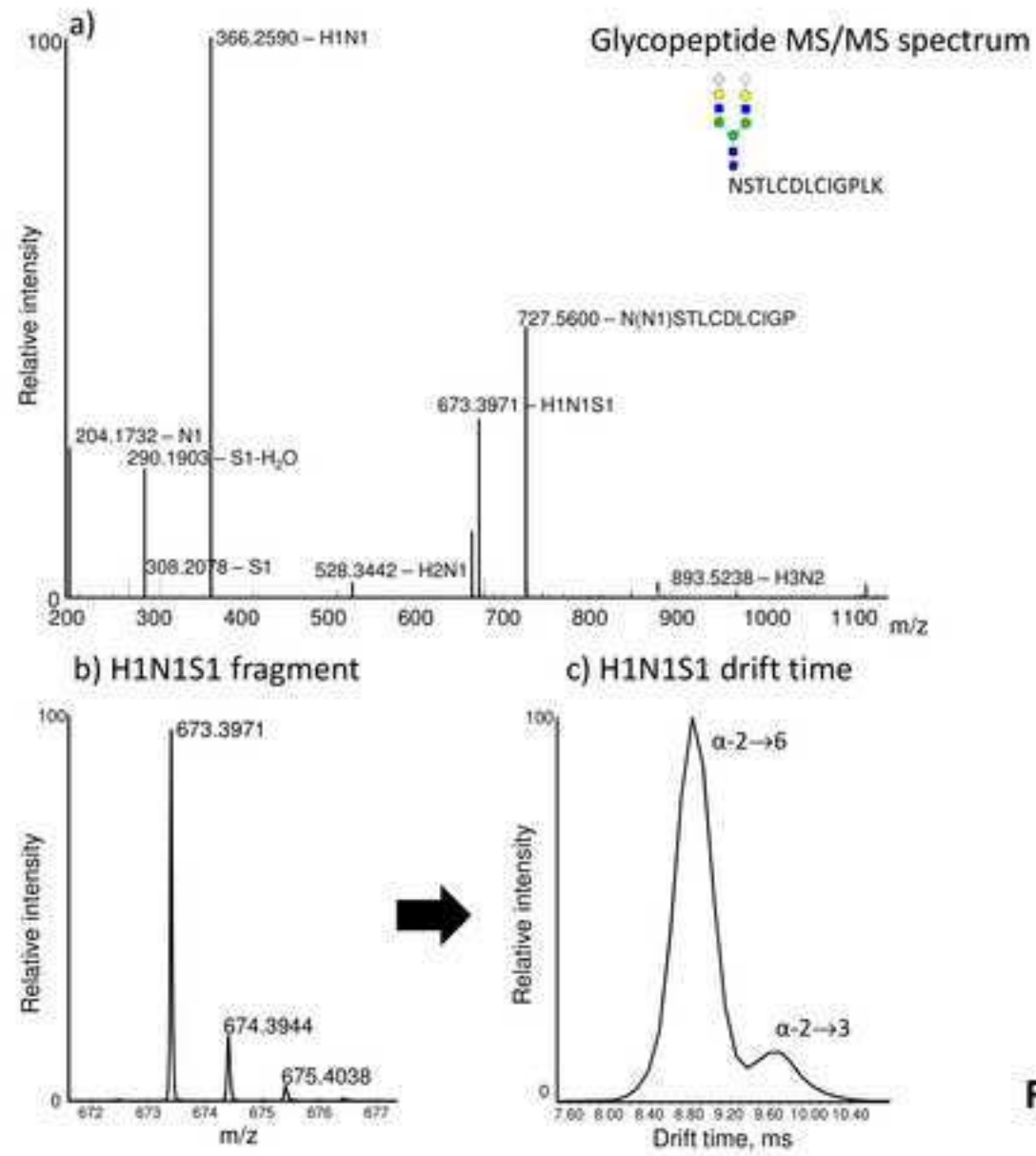**Click here to download high resolution image**
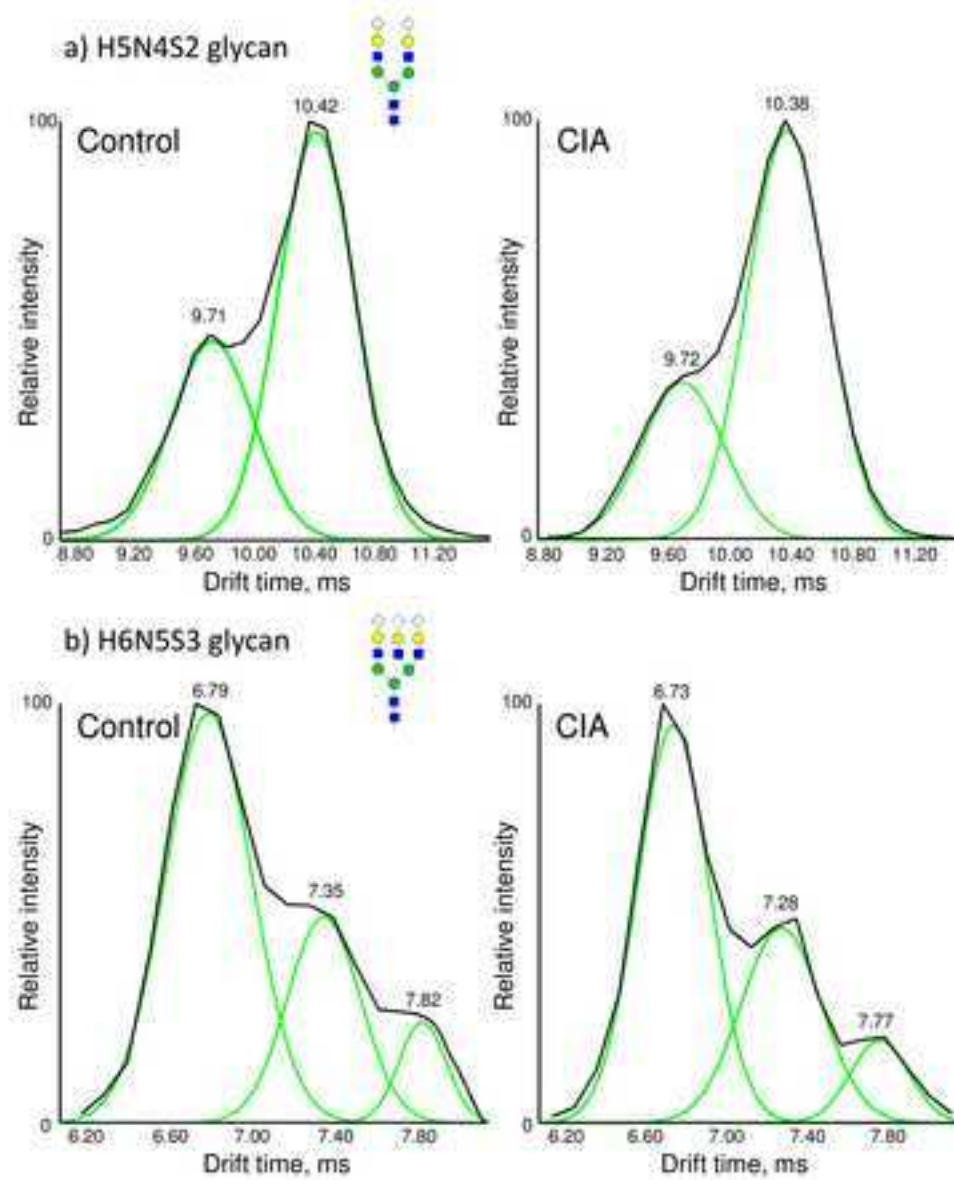
Figure 2

Figure 3

Figure 4

Supplementary material

*Conflict of Interest
Click here to download Conflict of Interest: The authors declare no conflicts of interest.docx